INDC-200

AERE - PR/NP 12

INDC(UK)*022/R

AERE - PR/NP 12

UNCLASSIFIED

E MINIMIS MAXIMA

United Kingdom Atomic Energy Authority

RESEARCH GROUP

NUCLEAR PHYSICS DIVISION PROGRESS REPORT

For the period 1st November 1966 to 30th April 1967

Editor: C. F. COLEMAN

Nuclear Physics Division,

Atomic Energy Research Establishment,

Harwell, Berkshire.

1967

000207

U.D.C.
539.1(047.1)

NUCLEAR PHYSICS DIVISION

PROGRESS REPORT

For the period 1st November 1966 to 30th April 1967

Editor: C. F. COLEMAN

Nuclear Physics Division,
U.K.A.E.A. Research Group,
Atomic Energy Research Establishment,
HARWELL.

August, 1967.

/HMB

HL 67/4257

CONTENTS

CONTENTS (cont'd)

NUCLEAR PHYSICS DIVISION

Division Head: Dr. B. Rose

IBIS 3 MV Pulsed Van de Graaff and 5 MV Van de Graaff

Dr. A. T. G. Ferguson

Tandem Generator

Dr. J. Freeman

Electron Linear Accelerator

Dr. E. R. Rae

Proton Physics

Dr. P. E. Cavanagh

Synchrocyclotron

Mr A. E. Taylor

Ion-Crystal Interactions

Dr. G. Dearnaley

Mössbauer Effect

Dr. T. E. Cranshaw

Miscellaneous Research

Dr. J. V. Jelley

INTRODUCTION

DR. B. ROSE

As this is the first introduction to be written to a progress report for the Nuclear Physics Division I shall not restrict myself completely to work carried out or completed in the last six months, and I shall allow myself a few generalities which would otherwise be out of place.

The division has two principal pursuits: to carry out measurements of nuclear data of importance in the reactor field and to undertake basic studies in nuclear physics. In addition, it has small programmes of work on the applications of the Mössbauer effect, on the interactions between fast ions and crystal lattices and on extensive air showers. It also provides facilities on its accelerators for other divisions of Harwell, for other research organizations and for some Universities, who have taken respectively 12%, 2% and 10% of the running hours in this half-year.

The reactor data work shows no sign of slackening, particular attention now being directed to the removal of discrepancies, to the improvement of accuracy in fission cross sections and in certain standard cross sections such as the lithium-6 and boron-10 capture cross sections and to the attempting of more sophisticated measurements than have yet been attempted anywhere, of which the measurement of α for ^{239}Pu is an example. The work on reactor spectra has now almost ceased at Harwell, and the discrepancy between the spectra from Vera assemblies as measured at Harwell and Aldermaston remains significant, despite some renormalization of the Harwell work. This discrepancy emphasizes the fact, which is frequently in danger of being overlooked, that the repeat of an experiment, even to the same, degree of accuracy, is not automatically "unnecessary duplication".

Of the basic work, probably the most important recent work has been the precision study of ft values of pure Fermi beta decays. This is still in progress, to re-examine one of two nuclei whose ft values are significantly different from the others. Another interesting development is the study of analogue resonances by observing the polarization of elastically scattered protons. Finally, a cooled image intensifier system developed in the division has proved very useful at the Royal Greenwich Observatory, Herstmonceux, applied to astronomical spectroscopy.

The items selected for mention in this introduction are in one sense arbitrarily chosen and it must not be assumed that other items not mentioned are inferior or even unfashionable. Study of the report will demonstrate, I believe, that the division's high standard of work is being maintained.

B. Rose

EDITORIAL NOTE

Since the results obtained from the various machines are no longer easily classified according to the energy of the charged beams, individual research items have been labelled with a single letter indicating on which machine the experiments were performed. These labels are as follows:-

Cockcroft Walton Generator (A. T. G. Ferguson)	A
3 MV pulsed Van de Graaff Generator IBIS (A. T. G. Ferguson)	B
5 MV Van de Graaff Generator (A. T. G. Ferguson)	C
13 MV Tandem Generator (J. M. Freeman)	D
45 MeV Electron Linac (E. R. Rae)	E
50 MeV Proton Linac : S.R.C.	F
Variable Energy Cyclotron : Chemistry Division	G
Synchrocyclotron (A. E. Taylor)	H
Nimrod Proton Synchrotron : S.R.C.	I

The running analyses for the various machines operated by the division are presented as far as possible in a uniform format, but some differences remain in the way in which the scheduling is arranged, and machines such as the Electron Linac can accommodate several experiments simultaneously.

NUCLEAR DATA FOR FAST REACTORS

(A) Elastic and inelastic neutron scattering from ^{239}Pu (D. A. Boyce, P. E. Cavanagh, C. F. Coleman, G. A. Gard, A. G. Hardacre, J. C. Kerr and J. F. Turner)

To check our absolute neutron cross section calibration against an accepted substandard we have interleaved over the energy range of our earlier measurements(1) observations of the 90° elastic scattering from our ^{239}Pu sample and from a carbon sample. Since substantial additions to the Maggie(2) Monte Carlo program would be required before it could be used to correct for the mutual shielding of the plutonium sample and its stainless steel can, we have preferred to take an approximate analytical method for multiple scattering corrections used by Cranberg(3), and to adapt this to our problem. This gives satisfactory agreement with measurements made on a tungsten sample with and without a similar can(4), and corrections for the plutonium sample are now being calculated.

The experimental program on neutron scattering from ^{239}Pu is virtually complete, apart from a proposed attempt to resolve scattering from the 8 keV level by making use of narrow resonances in Ca at 130 and 160 keV, and a report on the measurements is being prepared.

GENERAL REACTOR TECHNOLOGIES AND STUDIES

GENERAL NUCLEAR DATA FOR REACTORS

Fission cross section analysis (G. D. James and D. A. J. Endacott)

(a) Fluctuation analysis

Possible causes of the significantly high values of the serial correlation coefficient $r_k(W)$, first noted by Egelstaff(5) in an analysis of low energy fission cross section data and confirmed in a previous report(6), are being investigated. Three sets of resonance parameters each containing about 1700 levels have been generated by the program RMAT (by J. E. Lynn) in such a way that they have the same average properties as the ^{241}Pu resonance levels. Both single level Breit-Wigner and R-matrix fission cross sections and also their Doppler broadened values were calculated for the 3700 energy values in the range 17 eV to 1700 eV encountered in a typical time-of-flight measurement. The serial correlation coefficients $r_k(W)$ for the twelve sets of simulated fission cross section data show that (a), results for the R-matrix cross sections do not differ significantly from those for the single level Breit-Wigner cross sections (b), no significant change in $r_k(W)$ occurs when the cross sections are Doppler broadened and (c), the time-of-flight energy mesh does not lead to significantly high values of $r_k(W)$. By chance, one set of parameters gave some values of $r_k(W)$ above the 5% significance level. The cause of these high values will be investigated.

---

(1) A.E.R.E. report PR/NP 10, p. 1 (1966).

(2) Parker J. B., Towle J. H., Sams D., Gilboy W. B., Revnell A. D. and Stevens H. J. Nuclear Instrum. and Methods 30, 77 (1964).

(3) Cranberg L. Los Alamos report LA-2177 (1959).

(4) A.E.R.E. report PR/NP 9 (1966).

(5) Egelstaff P. J. Nuc. Energy 7, 35 (1958).

(6) James G. D. and Endacott D. A. J. Nuc. Phys. Div. Progress Report AERE - PR/NP 10, p. 1 (1966).

(b) Multilevel analysis of ^{239}Pu fission cross section near 85 eV

A comprehensive single level analysis of the ^{239}Pu total and fission cross sections below 250 eV has been reported by Derrien et al.[7]. At some energies several closely spaced wide single levels are required to explain the cross sections. When used in a multilevel formalism such levels would lead to large interference effects and produce cross sections incompatible with the data. A least squares multilevel fit to the fission cross section data of Derrien et al. over the energy range 78 eV to 88 eV has been made to determine the R-matrix parameters of the wide levels. All wide levels were assumed to have spin zero and the effect of the levels at 60.94 eV, 96.49 eV and 100.25 eV was taken into account. The cross sections calculated for three wide levels in a single fission channel occurring in the energy range 78 eV to 88 eV disagreed with the experimental data by factors as large as ten at some energies as a result of severe interference effects. It was found that a good fit to the data could only be obtained by omitting the wide level at 83.52 eV and by introducing a second fission channel for the spin zero levels. Fig. 1 shows by a solid line the multilevel fission cross section obtained from the parameters of Table I and also the data of Derrien et al. The parameters in Table I are as given by Derrien et al. except for the two levels at 81.37 eV and 85.13 eV and the absence of a level at 83.52 eV. At 60.94 eV, 96.49 eV and 100.25 eV the fission widths have been divided equally between the two fission channels.

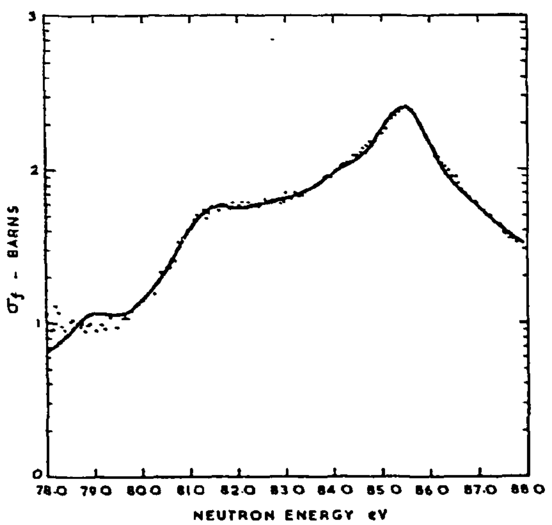

Fig. 1. Multilevel fit to ^{239}Pu fission cross section between 78.0 and 88.0 eV.

TABLE I

E_λ (eV)	Γ_n^0 (meV)	Γ_{f1} (meV)	Γ_{f2} (meV)	Γ_γ (meV)	J
60.95	3.843	2976	2976	40	0
78.95	0.012	140	-	40	1
81.37	0.527	−0.154	837.8	40	0
82.68	0.055	29.5	-	40	1
85.13	6.34	3157	−136.4	40	0
85.48	0.85	37.0	-	40	1
96.49	1.36	819	819	40	0
100.25	1.11	2976	2976	40	0

(H) Fission cross sections in the 20 keV to 20 MeV region (A. Langsford, M. S. Coates, D. B. Gayther, G. D. James and G. C. Cox)

An exploratory run to study the feasibility of fission cross section measurements on the synchrocyclotron has shown that:-

(a) With the present neutron intensities the counting rate is approximately one event per second in the fission detector and adequate for cross section measurements.

(7) Derrien H., Brons J., Eggermann C., Michaudon A., Paya D. and Ribon P. Proc. I.A.E.A. Conf. on Nuclear Data, Paris (1966). Paper CN-23/70 to be published.

(b) Backgrounds, measured by placing filters of boric oxide or aluminium in the beam, are at most 1 to 2% over the energy region.

(c) These counting rates and backgrounds roughly equal those in corresponding experiments on the Electron Linear Accelerator but the measurements can be made to higher energies and with better energy resolution.

(E) Neutron cross section measurements on sodium (M. C. Moxon, N. J. Pattenden, V. S. Brown and J. E. Jolly)

Continuing the work previously reported[8,9] further transmission measurements have been performed on another sample, a solution containing 0.214 g/ml of NaCl in heavy water enclosed in a silica cell. The measured minimum transmission at the 2.85 keV Na resonance peak was 0.098 ± 0.015, corresponding to an observed peak cross section of 350 ± 20 b. The corresponding figures for the other solution sample[9] were 0.34 ± 0.02 and 350 ± 25 b. Hence the previous results are confirmed, and further weight is given to the assignment J = 1 for this resonance.

(E) Neutron partial cross sections of ^{98}Mo, ^{100}Mo, ^{107}Ag and ^{109}Ag (A. Asami and M. C. Moxon)

Neutron scattering and capture measurements on ^{98}Mo and ^{100}Mo have been completed, but preliminary analysis of the results suggests that further measurements on much thinner samples of these isotopes may be required.

The results for ^{107}Ag and ^{109}Ag are now being analysed. Figs. 2 and 3 show the observed neutron capture cross sections for ^{107}Ag and ^{109}Ag respectively for neutrons in the energy range 100 eV to 200 eV. The isotopic assignment of the small resonances previously observed is clearly established.

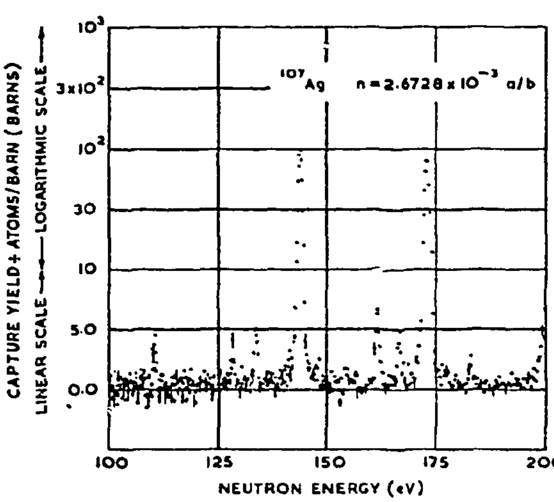

Fig. 2. Neutron capture yield from ^{107}Ag.

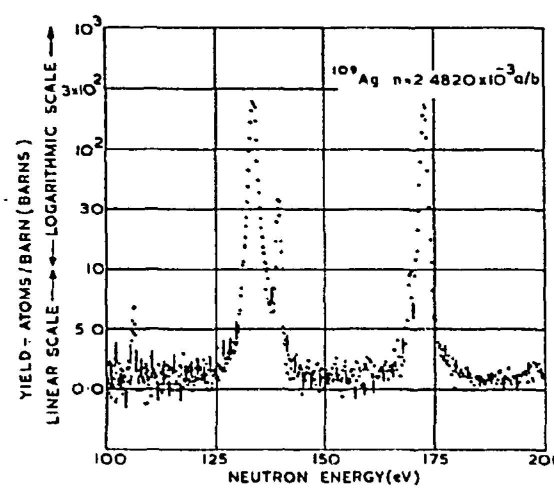

Fig. 3. Neutron capture yield from ^{109}Ag.

The rebuilding of the neutron scattering detector is nearly complete and preliminary measurements on lead and carbon samples indicate an improvement in the signal to background ratio for neutrons with

---

(8) Moxon M. C., Pattenden N. J., Brown V. S., Jolly J. E. and Pratt J. S. Nuc. Phys. Div. Progress Report AERE - PR/NP 11 (1967).

(9) Moxon M. C. and Pattenden N. J. The low energy neutron cross section of sodium. Proc. I.A.E.A. Conf. on Nuc. Data, Paris (1966), Paper CN-23/27.

energies above 1 keV. This improvement makes it feasible to measure the scattering cross sections of ^{10}B with reasonable accuracy in a reasonably short time, and such measurements will be carried out in the near future.

(E) Total cross section measurements on ^{6}Li and Au (K. M. Diment and C. A. Uttley)

1. Gold

The average neutron total cross section of gold has been measured between 7 keV and 7 MeV using the 120 m and 300 m spectrometers of the electron linear accelerator. The primary object was to determine the p-wave neutron strength function by the methods discussed in previous reports[10] and elsewhere[11]. The low energy s-wave potential scattering length $R'(= R(1 - R_0^\infty))$ and the distant level parameter R_0^∞ were determined separately by correcting the between resonance cross section obtained from thick sample, high resolution transmission measurements for the effects of local resonances, the parameters of which have been determined by Julien et al.[12]. However only some 30 resonances on each side of the chosen energy have been used to correct the observed potential scattering length so that the value of R_0^∞ obtained is uncertain because of the effects of local resonances which have not been resolved and measured. The variance $(\Delta R_0^\infty)^2$ which arises through considering only (m) resonances on either side of the chosen energy can be calculated in the uniform level density approximation to be

$$\overline{\Delta R_0^{\infty 2}} = 6\left(\frac{\lambda_0}{2R}\right)^2 S_0^2 \left(\frac{\pi^2}{6} - \sum_{r=1}^{m} \frac{1}{r^2}\right)$$

where λ_0 is the reduced neutron wavelength at 1 eV, R is the nuclear radius parameter $1.35A^{1/3}$ fm and S_0 is the s-wave neutron strength function Γ_n^0/D familiar in the experimental literature. Thus $(\Delta R_0^\infty)^2$ is large both when m is small and for those nuclei with large strength functions. Gold has a strength function in the range $(1.5 \rightarrow 2.0) \times 10^{-4}$, which is large compared with the values for nuclei in the 3P and 4P size resonances previously studied. As a result of the uncertainty in the distant level parameter (value − 0.127 ± 0.039) the potential scattering cross section of 9.85b is uncertain by ± .70 barns. Most of this uncertainty will be reflected, through the s-wave shape elastic scattering cross section, as an uncertainty in the p-wave compound nucleus cross section and therefore in the p-wave neutron strength function in the least squares fit to the total cross section below about 300 keV. Table II lists the average p-wave parameters S_1 and R_1^∞ and the s and d wave strength functions S_0, S_2 obtained from least squares fits to the total cross section between 7 keV and 1 MeV when the value of R_0^∞ is altered up or down by one standard deviation.

TABLE II

Average resonance parameters of Gold

R_0^∞	$S_0 \times 10^4$	R_0^∞	$S_1 \times 10^4$	$S_2 \times 10^4$
− 0.166	1.4	+ 0.081	0.38	0.93
− 0.127	1.53	+ 0.078	0.70	0.26
− 0.088	1.75	+ 0.109	1.27	− 0.12

(10) Uttley C. A. and Diment K. M. A.E.R.E. report PR/NP 10 (1966).

(11) Uttley C. A., Newstead C. M. and Diment K. M. I.A.E.A. Conference on Nuclear Data, Paris (1966). Paper CN-23/36.

(12) Julien J., De Barros S., Bianchi G., Corge C., Huynh V. D., Le Poittevin G., Morgenstern J., Netter F., Samour C. and Vastel R. Nucl. Phys. 76, 391 (1966).

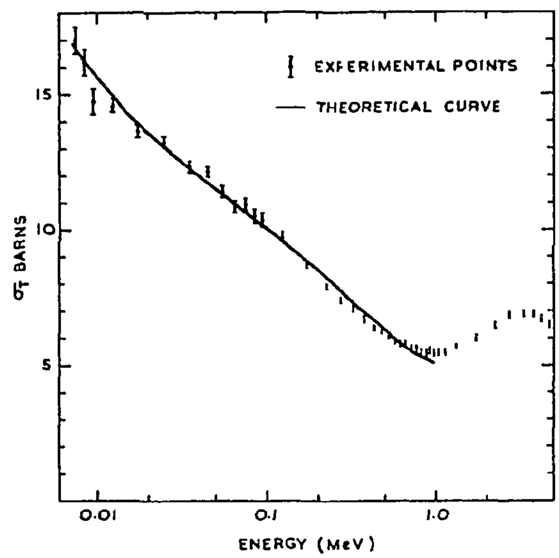

Fig. 4. Total cross section of gold.

In the fitting procedure it was assumed that $R_2^\infty = R_3^\infty = 0$ and $S_3 = S_1$. The fit to the data obtained using the observed value -0.127 for R_0^∞ is shown in Fig. 4. This fit leads to a value for the p-wave strength function of $(0.70 {}^{+0.57}_{-0.32}) \times 10^{-4}$. The large uncertainties should be considerably reduced when the thick sample average transmission data up to 50 keV have been analysed to determine R_0^∞ and, independently, S_1. The value for the p-wave strength function obtained here is significantly smaller than the predictions ($\sim 1.7 \times 10^{-4}$ and $\sim 1.5 \times 10^{-4}$) of the collective and spherical optical models respectively, and furthermore the parameters in row 1 of Table II associated with the low value of S_1 give the best fit to the experimental data.

2. Lithium 6

The total cross section of ^{6}Li is being measured, initially over the energy range 70 eV to 7 MeV, in an attempt to determine the extent of the $1/\sqrt{E}$ variation in the absorption cross section, the low energy scattering cross section, and the parameters of the 250 keV resonance. Three samples have been fabricated and canned in aluminium. The ^{6}Li to ^{7}Li ratio for these samples has been determined and they have been analysed for chemical impurities. The transmission measurements are alternated with further measurements on ^{10}B and ^{12}C. The preliminary data confirm the positions of the 2.08 MeV and 2.95 MeV resonances in carbon, but suggest that the peak of the p-wave resonance in ^{6}Li lies at about 247 keV, which is below the energy previously observed in the total cross section.

(E) The measurement of alpha, eta and the neutron cross sections of ^{239}Pu (B. H. Patrick, M. G. Schomberg and M. G. Sowerby)

Analysis of the data obtained in the two experiments in which eta and the fission and total cross sections of ^{239}Pu were measured has continued. The magnitude of the scattering cross section σ_s is of particular importance in this analysis both in correcting the fission cross section for the effects of multiple scattering and in determining the capture cross section σ_c from the formula

$$\sigma_c = \sigma_T - \sigma_F - \sigma_s , \qquad (1)$$

where σ_T and σ_F are the measured total and fission cross sections respectively. As described in the last progress report[13], the average fission cross section falls abruptly to about half of the expected value at ~ 600 eV, whereas the average total cross section shows little change. These facts cast doubts on the validity of the assumptions that the average elastic scattering cross section is energy independent and that the compound elastic part can be calculated from the s-wave strength function combined with averages of resonance parameters obtained from the resolved region below ~ 300 eV. This problem has been examined in detail and the results and conclusions are briefly described below.

In the energy region where only s-wave interactions are important (i.e. below ~ 10 keV) states with spin 0 and 1 contribute to the ^{239}Pu cross sections. Average cross sections have been calculated in 100 eV intervals from 100 eV to 1 keV and in 1 keV intervals up to 10 keV. In these calculations the

---

(13) Patrick B. H., Schomberg M. G. and Sowerby M. G. Nucl. Phys. Div. Progress Report AERE - PR/NP 11 (1967).

average resonance parameters of Derrien et al.[14] and the s-wave strength function values of Uttley[15] were used. It was assumed that the neutron widths Γ_n obeyed a Porter-Thomas distribution and the fission widths Γ_f were described by χ^2 distributions with two degrees of freedom for the spin 0 states and one degree of freedom for the spin 1 states[14]. The radiation width Γ_γ was taken to be constant. Using these distributions, the appropriate fluctuation factor was calculated in each case for the particular cross section being estimated. The calculations have shown that the fission cross section is divided almost equally between the two spin states whereas the scattering cross section is almost entirely due to the spin 1 states.

Now the sudden drop in the fission cross section at ~ 600 eV may be caused by (a) a change in one of the partial widths Γ_n, Γ_f or Γ_γ, (b) an increase in the level spacing (c) the opening of another exit channel, or a combination of any of these. The experimental evidence indicates that the fission cross section and the quantity $\frac{\sigma_F\sqrt{E}}{S_o}$ both fall but the total cross section is only slightly affected. The scattering data of Asghar[16] have been examined and although it is not possible to deduce absolute values, it is clear that there is no significant change in the scattering cross section in the region of 600 eV. By comparing the experimental evidence with the effects of the changes (a), (b) and (c) it is found that the only changes consistent with the experimental data are an increase in the spacing of the $J = 0$ levels or a decrease in the average neutron width Γ_n for these levels.

Since the compound elastic scattering takes place mainly through the spin 1 states we conclude that it is reasonable to calculate the compound elastic scattering cross section above 600 eV using averages of resonance parameters obtained from the resolved region below ~ 300 eV. The total scattering cross section is then obtained by adding the accurately measured value[15] of the shape elastic scattering cross section.

On this basis the capture cross section has been deduced from equation (1), and average values of alpha, the ratio of capture to fission cross sections, have been calculated at energies up to 10 keV, using the total cross section measurements of Uttley[15] and the fission cross section data of James[17]. The results indicate that alpha is about 1.0 from 600 eV to ~ 7 keV and then falls to ~ 0.6 at 10 keV.

(E) The direct measurement of alpha (E) for ^{239}Pu over the energy range 10 eV to 30 keV (M. G. Schomberg, M. G. Sowerby and F. W. Evans)

The quantity $\alpha(E)^*$ is of importance in fast reactor design, and a decision was taken some years ago to attempt a measurement of this quantity over the energy range 10 eV - 30 keV by making use of the Electron Linac with its boosted pulsed-neutron target and associated time of flight equipment. In order to carry out this measurement it has been necessary to develop a special detector system with the following main properties:-

(a) The ability to distinguish between radiative neutron capture and neutron induced fission events.

(b) A constant efficiency for the detection of radiative capture events irrespective of the form of the gamma ray cascade.

---

(14) Derrien H., Blons J., Eggerman C., Michaudon A., Paya D. and Ribon P. I.A.E.A. Conference on Nuclear Data, Paris (1966). Paper CN-23/70.

(15) Uttley C. A. EANDC(UK)40'L' (1964).

(16) Asghar M. EANDC(UK)70'S' (1967) Revised.

(17) James G. D. To be published.

*$\alpha(E)$ is the ratio of capture cross section to fission cross section at the neutron energy E.

(c) Adequate time resolution.

A neutron interaction resulting in fission generates a gamma ray cascade, of similar total energy to a radiative capture event, together with short range fission fragments and energetic fission neutrons. To distinguish between fission and capture events it is therefore necessary to observe either the fission fragments or the fission neutrons produced in fission in addition to the gamma rays generated in both fission and capture. The alpha activity of the ^{239}Pu and count rate considerations make it impracticable to detect fission fragments. A detector has therefore been constructed which can distinguish the energetic fission neutrons from scattered neutrons and gamma rays, and which also has the characteristics described in (b) and (c) above.

The detector, which is shown in section in Fig. 5, is a development of the system devised at C.B.M.N. Geel[(18)], which is itself an improved version of the Moxon-Rae detector[(19)]. It uses the

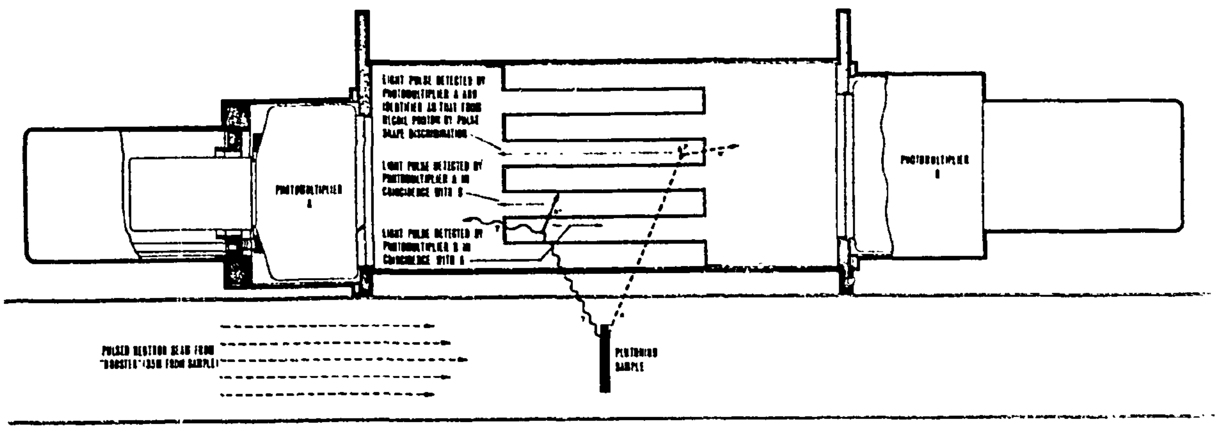

Fig. 5. A detector for the measurement of alpha (E).

liquid scintillator NE213. The main body of the counter is divided into two parts by means of a specially shaped aluminium separator, each part being viewed by its own photomultiplier. When the counter responds to fission neutrons each half acts as an independent system and pulse shape discrimination is used to distinguish recoil protons produced by neutron interactions within the scintillator from electrons produced by gamma ray interactions. As a capture detector it can be given an efficiency for the detection of radiative capture events independent of the nature of the resulting gamma ray cascade, in a similar fashion to the Moxon-Rae detector, by ensuring that the efficiency is proportional to the gamma ray energy - i.e. that $\frac{E_\gamma}{\epsilon(E_\gamma)}$ = constant, where E_γ is the gamma ray energy and $\epsilon(E_\gamma)$ is the efficiency at that energy. A fast coincidence is required between the outputs of the photomultipliers which view the two sides of the separator. As the energy of the incident gamma ray increases the number of secondary photons and recoil electrons produced also increases, while at the same time they are projected progressively more into the forward cone. By suitable design these facts can be exploited to make the probability of a coincidence increase linearly with gamma ray energy. The critical design features are the width of the separator divisions and the low energy bias on the phototube outputs. One must also consider the effect of the thin lead absorber which provides a low energy cut off, thus reducing the counting rate from the intense soft gamma ray background from the natural activity of the samples, which would otherwise disturb the operation of the pulse shape

---

(18) Carraro G. and Weigman H. EANDC(E)76 'u', p. 133.

(19) Moxon M. C. and Rae E. R. Nucl. Instr. Meth. 24, 445 (1963).

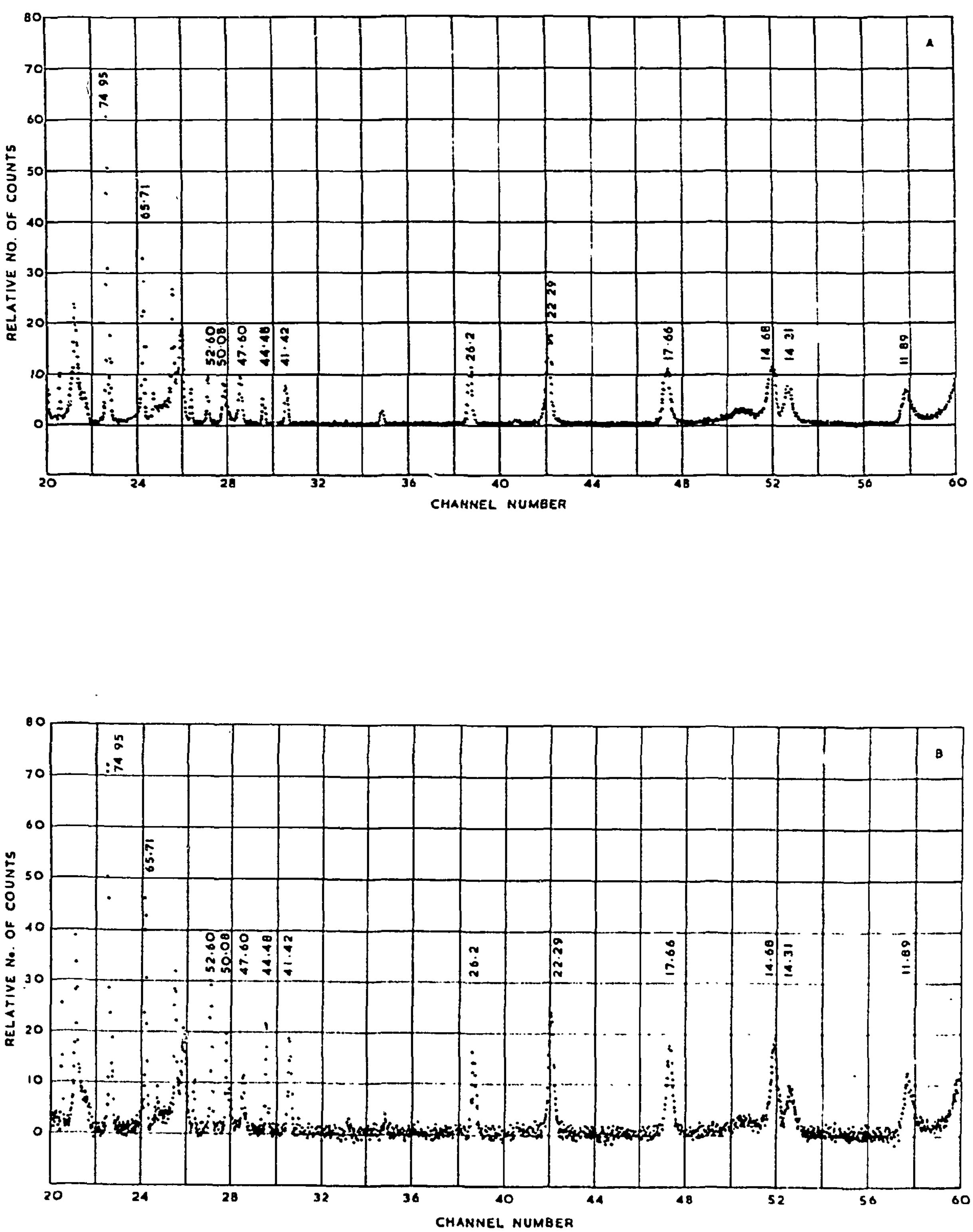

Fig. 6. Fission (A) and gamma-ray (B) counts per timing channel from a ^{239}Pu target.

discrimination system. Because the efficiency of the detector is small both for gamma rays and for neutrons the probability of neutrons and gamma rays from the same event being detected simultaneously is small. Many of the design calculations were performed using a Monte Carlo computer program written for this purpose by M. J. Hopper of the Theoretical Physics Division.

The detector is now operating, but some further work is necessary on the calibration and final adjustment of the gamma ray detection part of the system. Test results with ^{239}Pu, untreated except for background subtraction, are shown in Fig. 6, in which observed counts are plotted against neutron energy. If $N_f(E)\delta E$ is the number of fission events in the internal $E \rightarrow E + \delta E$ and $N_c(E)\delta E$ is the number of capture events, then the number of counts per unit energy interval from the neutron output of the detector, which is shown in the upper curve, is given by

$$n_f(E) \sim F_1 N_f(E)$$

and the number of counts per unit energy interval from the gamma ray output of the detector, shown in the lower curve, is given by

$$n_\gamma(E) \sim F_2 N_f(E) + F_3 N_c(E)$$

where F_1, F_2 and F_3 are constants determined by nomalisation. F_1 contains as a multiplying factor the quantity $\overline{\nu}(E)$, but experimental results on other materials suggests that the variation of this quantity from resonance to resonance is $\lesssim 4\%$.

The quantity alpha(E) can then be found from the equation

$$\text{alpha}(E) = \frac{N_c(E)}{N_f(E)} = \frac{\dfrac{n_c(E)}{n_f(E)} - \dfrac{F_2}{F_1}}{\dfrac{F_3}{F_1}}$$

These are only preliminary results, but even a cursory glance at, for example, the resonances at 52.60, 50.08, 47.60, 44.48 and 41.42 eV shows that alpha is varying noticeably from resonance to resonance.

(E) Determination of ^{240}Pu resonance parameters (M. Asghar, M. C. Moxon, N. J. Pattenden and J. E. Jolly)

The work reported previously[20] has been continued, and further transmission and capture measurements have been performed on additional samples. The thickest transmission sample contained 2.82×10^{-3} Pu atoms/b. Resonance analysis of the new measurements is proceeding. The sum of the number of resonances below a given energy as a function of energy is shown in Fig. 7 (overleaf). The total corresponds closely to that obtained at the Geel linac[21]. This indicates that in this region few resonances are missed due to our limited resolution, 2.5 ns/m compared with 0.9 ns/m used in the Geel measurements.

---

(20) Asghar M., Moxon M. C., Pattenden N. J., Jolly J. E. and Pratt J. S. Nuc. Phys. Div. Progress Report AERE - PR/NP 11 (1967).

(21) Bockhoff K. H. et al. Conference on Nuclear Data, Paris (1966). Paper CN-23/89.

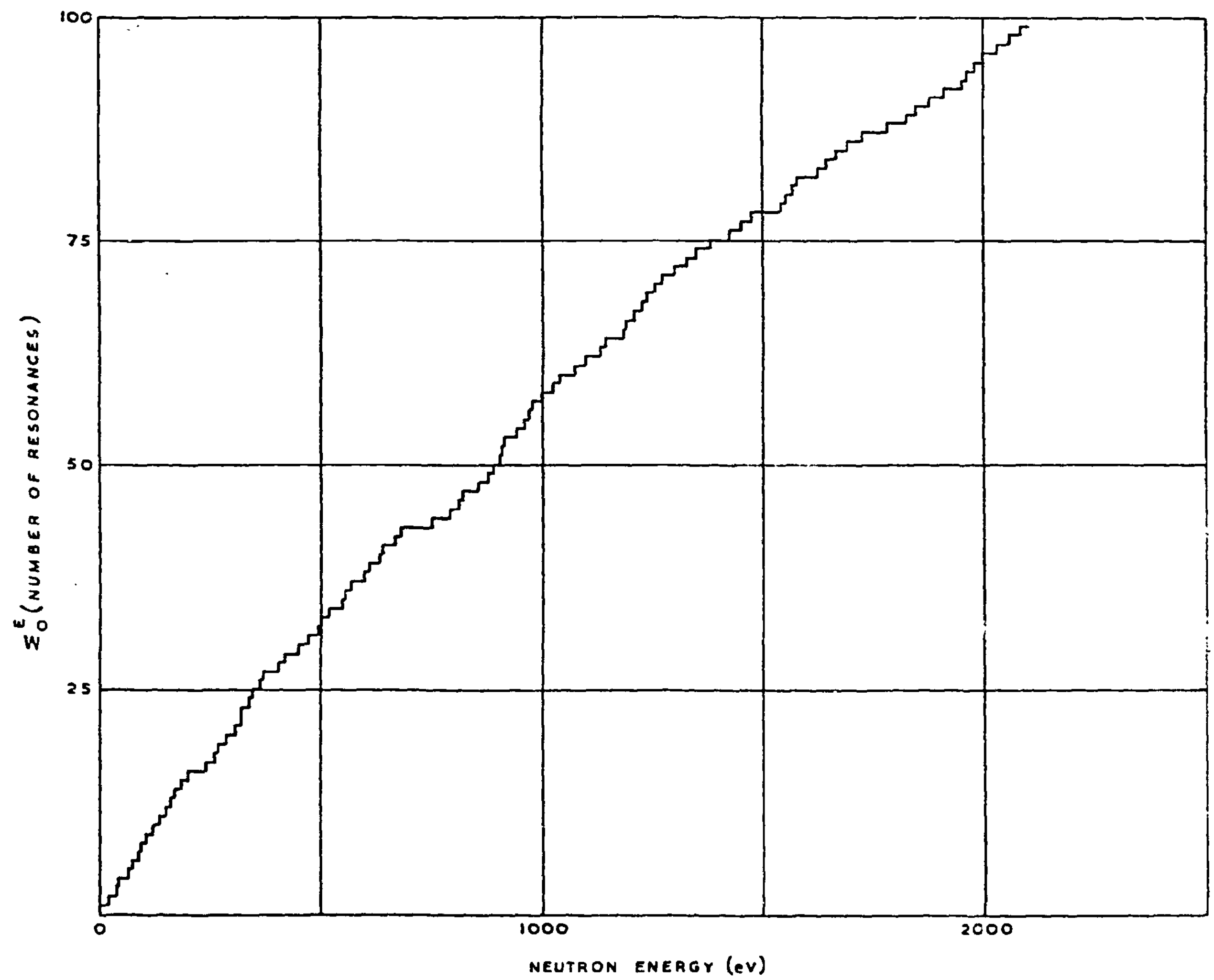

Fig. 7. Observed number of resonances below the energy E for ^{240}Pu.

Relationships between R-matrix and S-matrix reaction theories (J. E. Lynn)

A number of different formalisms are now available for the theoretical discussion of nuclear reactions. Perhaps the two most commonly used are the R-matrix theory of Wigner and Eisenbud[22] and the S-matrix theory of Humblet and Rosenfeld[23]. The former employs, as a basic set for its expansions, the eigenvalues and eigenfunctions of the nuclear hamiltonian within an internal region bounded by specified channel radii and constrained by real, energy independent boundary conditions. These channel radii and boundary conditions have been criticized by the S-matrix school as being artificial and arbitrary. The S-matrix expansions are about the poles of the collision matrix in the complex energy plane. A simple physical interpretation of these poles identifies them with radioactive decaying states. The two theories have their own advantages and disadvantages. The R-matrix theory can be cumbersome to handle in computations, particularly in computations of average cross sections, and the interpretation of its parameters is not always straightforward. On the other hand it gives expressions for the collision

---

(22) Wigner E. P. and Eisenbud L. Phys. Rev. 72, 29 (1947).

(23) Humblet J. and Rosenfeld L. Nuclear Physics 26, 529 (1961).

matrix which are unitary in form; this is an important property that provides for the conservation of flux in the stationary wave representations of the nuclear reaction. The S-matrix theory is simpler to handle in computations, and the individual terms of the expansion can be immediately interpreted as resonance forms. It does, however, have more parameters than the R-matrix theory, and this immediately implies (since both theories must describe the same collision matrix) that some of its parameters are redundant, or, in other words, are correlated with the others. This brings out the most fundamental difficulty of this theory, namely, that the expression for the collision matrix is not unitary in form. This imposition of unitarity governs the correlations among the parameters, and introduces difficulties into the practical use of the theory which are not immediately apparent in its simple form. Part of our work is directed towards a better understanding of the relationships between the two theories.

A number of nuclear cross section data have been analysed in the S-matrix formalism, and often striking agreement has been obtained between the data and the fitted curve. This agreement has been used as evidence of the validity of the S-matrix theory. However, to our knowledge, no attempts have been made to reconcile such fitting procedures with the demands of unitarity, and it is therefore worth taking a closer look at such fits. A particularly good example is the two-level fit by Mahaux[(24)] to the $^{15}N(p,\alpha_0)$ reaction to 1.1 MeV. His fit employed seven parameters and is very good. We have fitted the same data with a two-level approximation from R-matrix theory. The fit is every bit as good as if not better than Mahaux's, and it employs only six parameters. As we have explained, these parameters give a collision matrix that is unitary, and it is possible to transform this particular collision matrix into the S-matrix form in order to find a "unitary" set of S-matrix parameters. This has been done and the resulting set differs very considerably from Mahaux's set (for many parameters by several times the statistical error allowable by the R-matrix fit). Studies are also being made of the $^{51}V(n,n)$ reaction at energies up to 25 keV. In this case with two non-zero spins the extra freedom of the S-matrix theory (ignoring unitarity) makes it extremely difficult to obtain a satisfactory determination of the background parameters, although the equivalent R-matrix parameters were found quite ambiguously some years ago[(25)].

We have also begun to study the statistical properties of S-matrix parameters. For this purpose two computer programmes have been written. Both start from a given set of R-matrix parameters. One is used to find the poles of the collision matrix that can be generated from this set, and the other performs numerical contour integrations around these poles to find their factorised residues (the "partial widths"). The first case to be considered is a 60-level example simulating low energy neutron-induced fission through a single fully open statistical model channel. Through such studies it is hoped to obtain statistical distributions and correlations of parameters so that one can compute, among other things, theoretical average cross sections.

PDP-4 data processor (E. M. Bowey, G. B. Dean and J. L. Wilbourn)

The computer operated for 1380 hours during this period. The main processor has operated satisfactorily at all times, but some delays have occurred through failure of peripheral equipment.

---

(24) Mahaux C. Nuclear Physics 71, 241 (1965).

(25) Firk F. W. K., Moxon M. C. and Lynn J. E. Proc. Phys. Soc. 82, 477 (1963).

(E) The energy dependence of the $^6Li(n,\alpha)^3He$ cross section in the energy range 10 eV to 100 keV (M. S. Coates, K. M. Diment, D. B. Gayther, B. H. Patrick, M. G. Schomberg and M. G. Sowerby)

We have continued our investigation of the energy dependence of the $^6Li(n,\alpha)$ cross section through the comparison of neutron spectra measured with detectors making use of the $^6Li(n,\alpha)$ and $^{10}B(n,\alpha)$ reactions respectively, assuming a $1/v$ dependence for the latter reaction. The emphasis has been placed on the region below 30 keV and the question whether or not the cross section follows the $1/v$ law. Shapiro[26] showed that the s-wave parts of the $^6Li(n,\alpha)$ and $^{10}B(n,\alpha)$ cross sections cannot show a strict $1/v$ energy dependence, but are more correctly written as

$$\sigma = \text{const. } E^{-1/2} + \Lambda\sigma + \beta E^{1/2} + \ldots$$

where the first term represents the $1/v$ law, the constant term $\Lambda\sigma$ is determined only by the absorption cross section at zero energy and the spin of the reaction channel, and β is a constant determined by the states of the compound nucleus excited by s-wave neutrons. Bergman and Shapiro[27] show that for ^{10}B $(\Lambda\sigma)_B = -0.40 \pm 0.03$ barn, and deduce that $(\Lambda\sigma)_{Li} = -0.03 \pm 0.01$ barn. Since there are no s-wave levels in ^7Li close to the neutron binding energy, β will be very small. However for $^{10}B(n,\alpha)$ $\beta E^{1/2}$ is expected to be significant where the cross section is low, and it is probably this fact which maintains the $^{10}B(n,\alpha)$ cross section at approximately the $1/v$ level up to $\sim$ 100 keV[28]. These terms have not been taken into account in our present calculations, in which we have so far assumed that the $^{10}B(n,\alpha)$ cross section is proportional to $1/v$.

The Monte Carlo programme of Lynn[29] which was used to calculate multiple scattering corrections to the lithium glass data has been checked against the Gem code at Risley[30]. It has been found that the results from the two programmes agree within 2%.

A further determination of the $^6Li(n,\alpha)$ cross section between 50 eV and 30 keV has been made using the "no sample" data obtained in a transmission measurement on the 97 m flight path. The data were treated in the same way as the data for thin lithium glass described in the last progress report[31]. The detector was a lithium glass disc 1 inch thick and 2½ inches in diameter coupled to a photomultiplier by a ½ inch thick Perspex light guide, the symmetry axis of the system lying along the direction of the neutron beam. The Gem code was used to calculate the multiple scattering corrections for neutrons interacting in the lithium glass and in the light guide. With this system the correction varied from 25% at 50 eV to $\sim$ 200% at 30 keV. Even with this extremely large and rapidly varying correction the results for the $^6Li(n,\alpha)$ cross section agreed with those deduced from the ⅛ inch thick glass specimen within $\sim$ 10% at 30 keV. Although the thick glass data will not be used in the final calculation of the $^6Li(n,\alpha)$ cross section, the fact that the results are in good agreement with those from the thin glass specimen adds to our confidence in the validity of the corrections.

---

(26) Shapiro F. L. Soviet Physics JETP 34, 1132 (1958).

(27) Bergman A. A. and Shapiro F. L. Soviet Physics JETP 13, 895 (1961).

(28) Spaepen J. I.A.E.A. Conference on Nuclear Data, Paris (1966). Paper CN-23/119.

(29) Lynn J. E. Private communication.

(30) Hart W. Private communication.

(31) Coates M. S., Diment K. M., Gayther D. B., Patrick B. H., Schomberg M. G. and Sowerby M. G. Nucl. Phys. Div. Progress Report AERE - PR/NP 11 (1967).

The effects of the resonance at ~ 255 keV on the $^6Li(n,\alpha)$ cross sections below 100 keV have been calculated using the resonance parameters of Bergstom et al.[32]. At present if the $^{10}B(n,\alpha)$ cross section is assumed to be proportional to $^1/v$ the data show that the $^6Li(n,\alpha)$ cross section is consistent with a $^1/v$ term plus the tail of the resonance.

(E) Time of flight neutron spectrum measurements on a sub-critical fast reactor assembly (M. S. Coates, D. B. Gayther and P. D. Goode)

Preliminary data have been presented[33] from an experiment in which the neutron spectrum emerging from the centre of a sub-critical VERA 7A assembly was measured using the pulsed source time of flight method on the 45 MeV electron linac. This spectrum has now been re-evaluated with a more reliable efficiency calibration for the ^{10}B-Vaseline plug[34] used in the measurements. Previously the response (relative detection efficiency) below 100 keV was obtained by comparison with a thick ^{10}B-plug the response of which had been calculated from a Monte Carlo program. In this case the calculation could be in error since multiple scattering effects were evidently important, and these would be sensitive to uncertainties in the ^{10}B scattering cross section. In consequence a further comparison has been made with a much thinner ^{10}B-plug, in which the effects of multiple scattering are small enough for corrections to be applied with confidence. The measurements were made in the energy range 160 eV to 200 keV by the time of flight method, using the electron linac as a primary neutron source, and two different flight paths. The $^{10}B(n,\alpha)$ cross section is assumed to varry in this region as $^1/v$. Available experimental evidence[35] indicates that this assumption is correct to about ± 5% up to at least 100 keV, although theoretically a strict $^1/v$ dependence cannot be justified[36]. Since the detector observes the γ-rays from the first excited state of ^7Li produced in the (n,α) reaction, allowance was made for the slight change (4%) in the branching ratio $^{10}B(n,\alpha_1)^7Li^*/[^{10}B(n,\alpha_0)^7Li + {}^{10}B(n,\alpha_1)^7Li^*]$ between 80 keV and 200 keV[37]. The response curve is shown in Fig. 8 (overleaf). The absolute efficiency is obtained by normalising to the high energy data obtained on the pulsed Van de Graaff IBIS using the technique previously described[38]. The normalisation was made in the region of 100 keV, but it was found that within the accuracy of the measurements the energy variation of the detector efficiency in the range 100 → 200 keV, assuming a $^1/v$ variation in the $^{10}B(n,\alpha)$ cross section, was in agreement with the IBIS measurements. The structure in the response curve at 35, 90 and 150 keV is due to resonances in the 0.5 mm Al can which contains the ^{10}B-Vaseline mixture; the detailed behaviour in this region was obtained with higher energy resolution than is indicated by the experimental points in the figure. The results show that an overall error of about 10% was present in the theoretically extrapolated response used previously.

The re-evaluated VERA 7A spectrum shown in Fig. 9 (overleaf). The spectrum has been corrected for the experimental resolution using an iterative procedure which makes use of the measured shape of the neutron pulse in the assembly. This correction was only significant above 500 keV and had a maximum value of 10% at 3 MeV. A correction has also been applied for the effect of neutron slowing down which causes the slower neutrons to leave the assembly later than the faster ones. The magnitude of the effect was determined from the apparent shifts in the energies of known resonances in Mn and Fe (constituents of the stainless steel fuel element containers) - and gave rise to a barely significant

(32) Bergstrom A., Schwarz S., Stromberg L. G. and Wallin L. CCDN-NW 3, p.7 (1966).

(33) Coates M. S., Gayther D. B., Goode P. D. and Tripp D. J. Nuc. Phys. Div. Progress Report AERE - PR/NP 11 (1966).

(34) Coates M. S., Gayther D. B., Goode P. D. and Tripp D. J. Nuc. Phys. Div. Progress Report AERE - PR/NP 10, p. 22 (1966).

(35) Spaepen J. Paper CN23/119, Proc. I.A.E.A. Conf. on Nuclear Data, Paris (1966).

(36) Coates M. S., Diment K. M., Gayther D. B., Patrick B. H., Schomberg M. G. and Sowerby M. G. This report.

(37) Mooring F. P., Monahan J. E. and Huddleston C. M. Nuc. Phys. 82, 16 (1966).

(38) Gayther D. B. and Goode P. D. Nuc. Phys. Div. Progress Report AERE - PR/NP 7, p. 14 (1964).

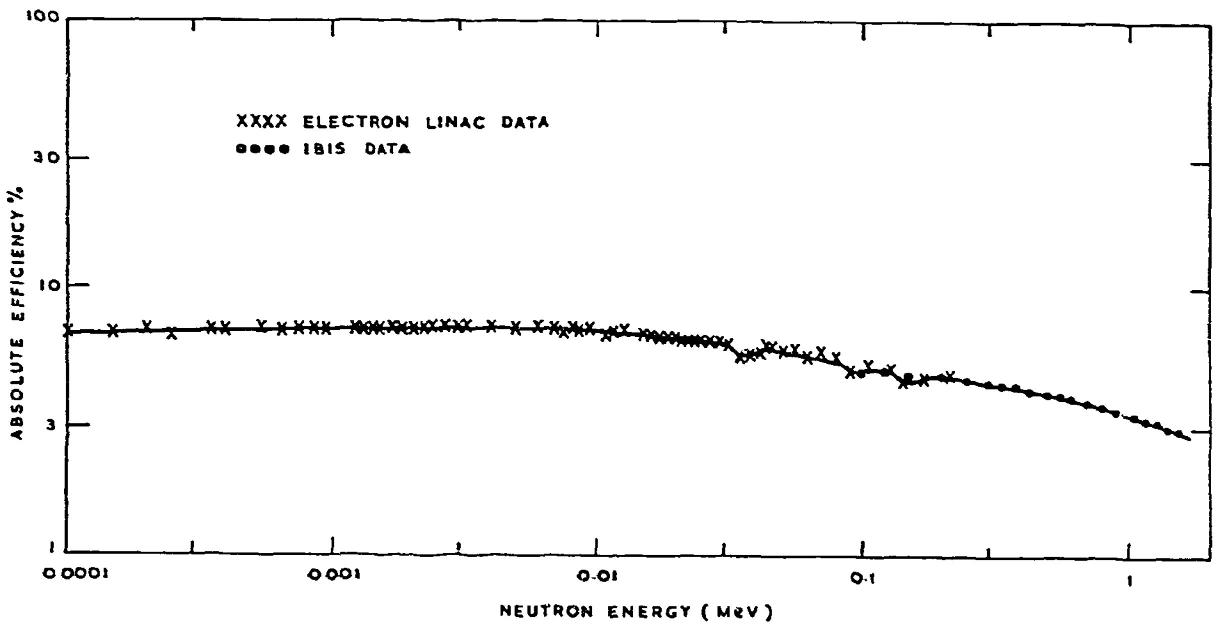

Fig. 8. B-vaseline plug energy response.

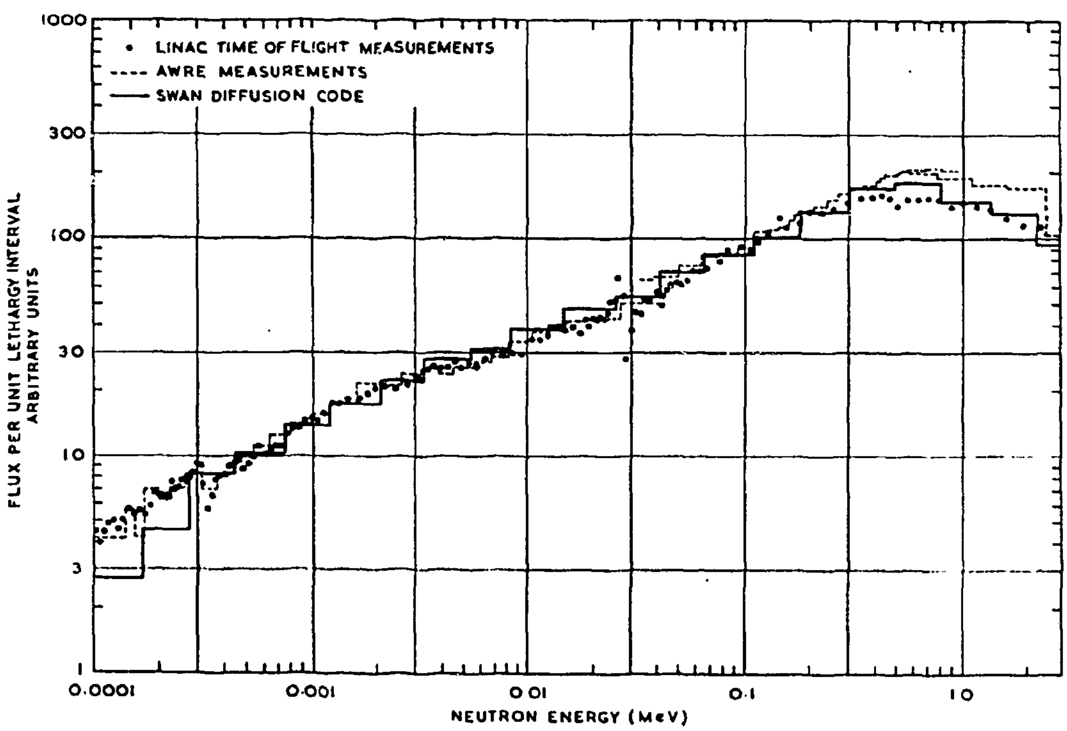

Fig. 9. Re-evaluated spectrum measurements on a VERA 7A assembly.

change in the shape of the spectrum. Fig. 9 also shows the spectrum determined in a similar assembly at A.W.R.E. using the composite technique(39), together with a 35 group SWAN calculation made for the critical system using FD2(R) nuclear data. The linac data and the composite data have the same shape in the region below 80 keV, and in the figure they have been normalised to one another. This is the energy region which was covered by the time of flight technique in the composite measurement. However at higher energies the linac spectrum is still considerably softer than the A.W.R.E. experimental data, although only slightly softer than the theoretical spectrum. The cause of the discrepancy between the two experiments is not yet resolved. The A.W.R.E. measurements are to be repeated and it is also hoped to investigate theoretically possible perturbations arising from differences between the various techniques. Probably the most important of these will be the dependence of the shape of the spectrum on the value of k_{eff}. The A.E.R.E. measurement was made on a sub-critical system, while in the composite technique the system was critical for measurements made at energies greater than 50 keV and sub-critical for measurements below this energy. A detailed account of the A.E.R.E. measurements will be published shortly(40).

(E) Measurements of fast neutron spectra in reactor materials (M. S. Coates, D. B. Gayther and P. D. Goode)

The series of time of flight measurements of fast neutron spectra in geometrically simple arrays of pure materials has been completed. The measurements are intended to provide a basis for comparison with reactor calculations using specific nuclear data in well defined and easily calculable conditions. Table III lists the measurements which have been made. The experimental arrangement and preliminary

TABLE III

Materials and Geometrical Arrangements used to study Fast Neutron Spectra

Material	Shell Outside Diameter (cm)	Shell Wall Thickness (cm)	Radial Distance of measurement point from outside of shell (cm)	Angle of Beam to Radius Vector (deg.)
Natural Uranium	23.9	6.1	0.0	0
	23.9	6.1	0.0	45
	28.4	8.4	0.0	0
	28.4	8.4	0.0	45
	28.4	8.4	4.3	0
	32.0	11.5	0.0	0
	32.0	11.5	0.0	45
Graphite	40.6	15.2	0.0	0
	40.6	15.2	0.0	45
	40.6	15.2	10.2	0
	40.6	15.2	5.2	0
Sodium	90.7	41.6	0.0	0
Polythene	20.3	5.1	0.0	0
	20.3	5.1	0.0	45

(39) Weale J. W., Benjamin P. W., Kernshall C. D., Paterson W. J. and Redfearn J. Berkeley Conf. on Radiation Measurements (1966).

(40) Coates M. S., Gayther D. B., Goode P. D. and Tripp D. J. A.E.R.E. Report R 5330 (1967).

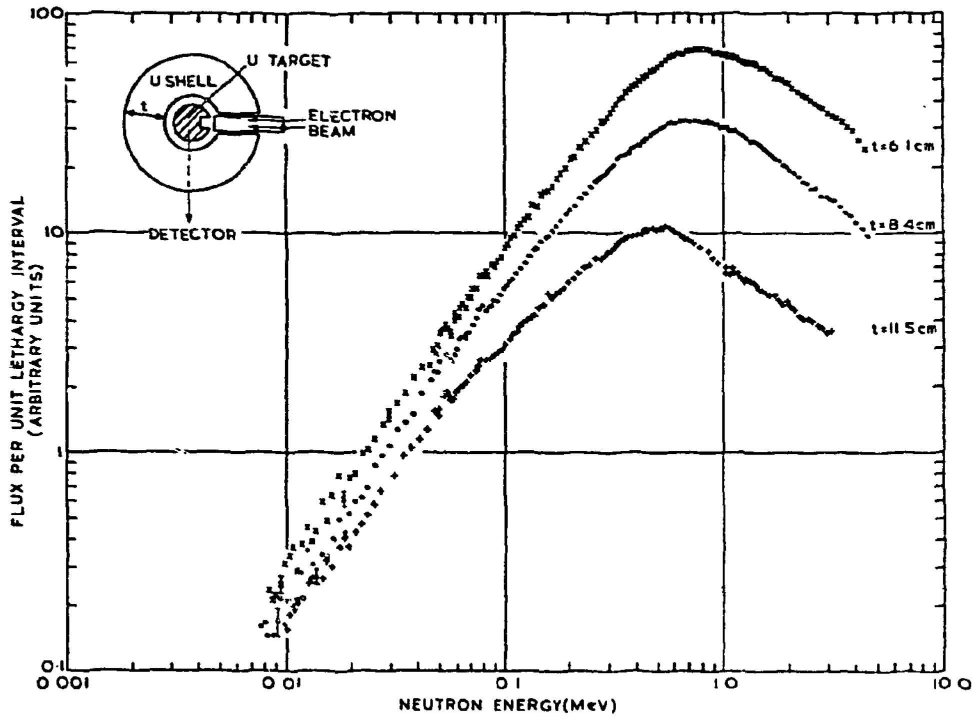

Fig. 10a. Measured 0° leakage spectra from natural uranium shells.

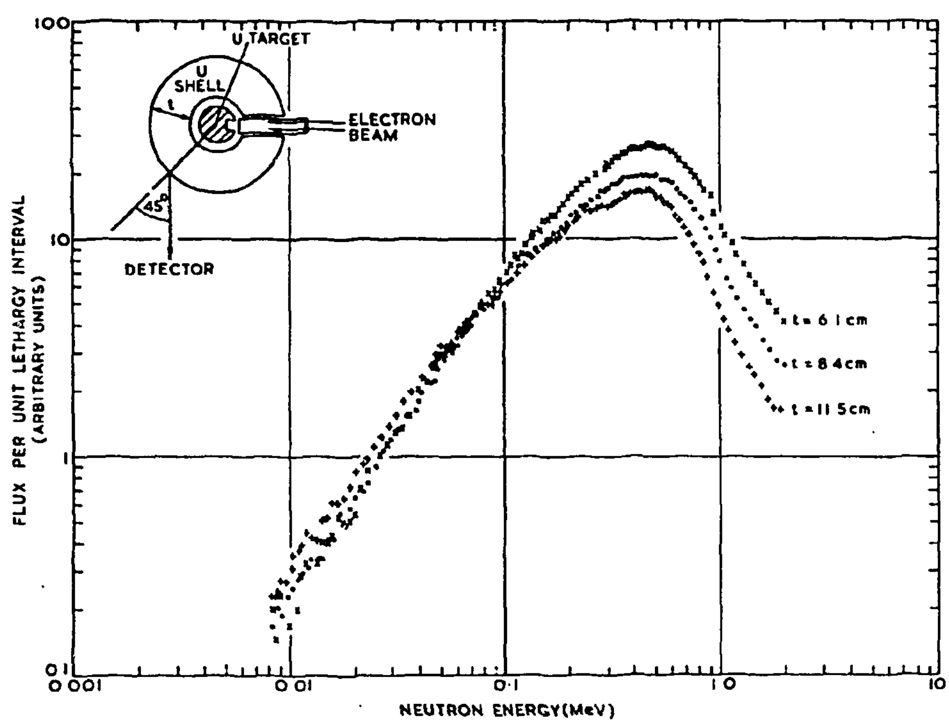

Fig. 10b. Measured 45° leakage spectra from uranium shells.

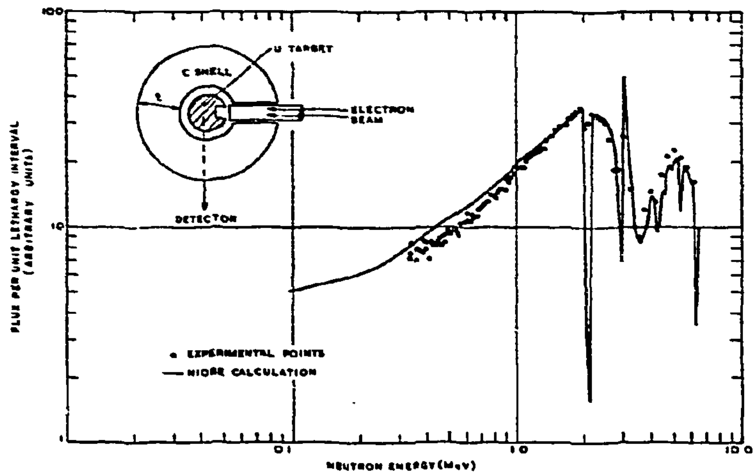

Fig. 11. Measured and calculated 0° leakage spectrum from a graphite shell.

spectra have been reported previously(41). The materials were used in the form of spherical shells with a central nearly isotropic source of fast neutrons of known energy distribution(42). We measured the energy spectra of beams of neutrons emerging from small areas on the surface of the shell (leakage) and at particular depths within the shell, the beams making angles of either 0° or 45° to the radius vectors at the appropriate points. Analysis of the experimental data is now almost complete and the work is to be published(43). Calculations for comparison with the experimental spectra are in progress. Carlson Sn calculations are being carried out by E. D. Pendlebury (A.W.R.E.) and A. F. Avery (Shielding Group) is providing calculations using the NIOBE code.

Fig. 10 shows the leakage spectra for the three uranium shells at 0° and 45° to the radius vector and Fig. 11 shows a comparison of a NIOBE calculation on graphite with the high energy part of the experimental spectrum.

FUNDAMENTAL AND BASIC RESEARCH

(B) Studies of various (^3He,n) reactions (J. M. Adams, A. Adams (Manchester) and J. M. Calvert (Manchester))

This series of experiments(44) has been concluded with a further investigation of the $^{20}Ne(^3He,n)^{22}Mg$ reaction, using a ^{20}Ne gas target, and employing a 0.00002 in. Ni foil window to minimise the energy lost by the ^3He ions in entering the gas cell. The present study of extremely proton-rich nuclei by means of (^3He,n) reactions has included ^{12}N, ^{16}F, ^{22}Mg and ^{26}Si. Generally speaking our results, which are summarised in Table IV (overleaf), agree very well with similar work done recently in other laboratories(45,46,47), but are more precise.

---

(41) Gayther D. B. and Goode P. D. Nuc. Phys. Div. Progress Report AERE-PR/NP 10, p. 20 (1966).

(42) Gayther D. B. and Goode P. D. A.E.R.E. Report R 5331 (1966).

(43) Coates M. S., Gayther D. B. and Goode P. D. A.E.R.E. Report R 5364 (1967).

(44) Adams J. M., Adams A. and Calvert J. M. A.E.R.E. Report PR/NP 8-10.

(45) Zafiratos C. D., Ajzenberg-Selove F. and Dietrich F. S. Nuc. Phys. 77, 81 (1966).

(46) Zafiratos C. D., Ajzenberg-Selove F. and Dietrich F. S. Phys. Rev. 137, B1479 (1965).

(47) McMurray W. R., Van der Merwe P. and van Heerden I. J. Nuc. Phys. A92, 401 (1967).

TABLE IV

The Nuclei ^{12}N, ^{16}F, ^{22}Mg and ^{26}Si

Reaction	Level	Q-value[a] (MeV)	Excitation (MeV)	Residual Mass[a] (Amu ± microamu)	Mass excess[b] (MeV)
$^{10}B(^{3}He,n)^{12}N$	g.s. 1 2	1.574 ± 0.007	0 0.969 ± 0.010 1.191 ± 0.010	12.018613 ± 8	17.338 ± 0.008
$^{14}N(^{3}He,n)^{16}F$	g.s. 1 2 3	−0.970 ± 0.015	0 0.253 ± 0.035 0.422 ± 0.015 0.711 ± 0.015	16.011480 ± 15	10.693 ± 0.015
$^{20}Ne(^{3}He,n)^{22}Mg$	g.s. 1	0.197 ± 0.025	0 1.06 ± 0.04	21.999593 ± 25	−0.379 ± 0.025
$^{24}Mg(^{3}He,n)^{26}Si$	g.s. 1	0.095 ± 0.015	0 1.809 ± 0.015	25.992305 ± 15	−7.168 ± 0.015

(a) ^{10}B, ^{14}N, ^{20}Ne, ^{24}Mg, ^{3}He and n atomic masses taken from the 1964 Mass Tables[49].

(b) Based on ^{12}C = 12.000000 amu and a conversion factor of 1 amu = 931.476 MeV.

In addition angular distributions for the $^{14}C(d,n)^{15}N$ reaction have been measured at an incident deuteron energy of 3.0 MeV for comparison with the distributions obtained previously for the $^{13}C(^{3}He,n)^{15}N$ and $^{14}N(d,n)^{15}O$ reactions[44]. It was found possible to observe neutron groups corresponding to excitations in ^{15}N of up to 10.0 MeV.

The DWBA analysis of the reactions leading to ^{15}O and ^{15}N and of the $^{9}Be(^{3}He,n)^{11}C$ and $^{10}B(d,n)^{11}C$ reactions[44], has now been completed. We used a new version of a computer program based on the theory of Rook and Mitra[48] for two nucleon stripping reactions. This program can also be used for one nucleon stripping calculation.

(B) The measurement with a Ge(Li) spectrometer of gamma-rays following inelastic neutron scattering (B. H. Armitage, T. Braid*, A. T. G. Ferguson, G. C. Neilson+ and W. Pritchard≠)

In an attempt to exploit the improved gamma-ray energy resolution offered by Ge(Li) detectors we have begun a programme of measurements on the de-excitation gamma-rays following inelastic scattering of fast neutrons. We used the nanosecond pulsed beam system of IBIS with time of flight gating to reduce the effective neutron induced backgrounds in a 30 cc. Ge(Li) detector. A time resolution of 6 ns has been obtained with gamma-rays of 0.5 MeV and above, using a time compensation system in which the output of the time-to-pulse-height converter is mixed with a compensation pulse obtained from the output of a second time-to-pulse-height converter in which the "start" and "stop" pulses are derived from the fast pulse by means of two discriminators set at "low" and "high" levels respectively. At gamma-ray energies greater than 0.5 MeV the application of this time compensation system has decreased the time resolution from 30 ns to 6 ns.

---

(48) Rook J. R. and Mitra D. Nuc. Phys. 51, 96 (1964).

(49) Mattauch J. H. E., Thiele W. and Wapstra A. H. Nuc. Phys. 67, 1 (1965).

*On leave from Argonne National Laboratory.

+On leave from University of Alberta.

≠On attachment from University of Exeter.

Gamma-ray spectra have been obtained from samples of about 200 gm of natural U and natural Th at several neutron energies between 1 and 2 MeV, using a tritium target and a 50 cm flight path. Analysis of the data is not yet complete and as might be expected the spectra are rather complex.

Estimate of neutron widths of the 2^- and 3^- analogue states in ^{90}Zr decaying to the $\frac{1}{2}^-$ (0.59 MeV) state in ^{89}Zr and the parameters of the analogue resonances (A. M. Lane and S. Ramavataram)

A qualitative description of the decay of the lowest analogue states in ^{90}Zr was given in an earlier report[50]. Assuming no configuration admixture in the ^{90}Y ground state we indicated that decay to the ground state of ^{89}Zr could only be explained by invoking complicated configuration admixtures in the final state.

On the other hand for the 2^- and $3^- \rightarrow \frac{1}{2}^-$ transitions configurational overlaps between initial and final states permit us to estimate the neutron width of these analogue resonances. Since the analogue state wave function ϕ_0 is a linear combination of $\chi_{9/2}$, $\chi_{5/2}$ and $\chi_{1/2}$ in ^{90}Zr we expect two T = 5 states represented by ϕ_1 and ϕ_2 to be admixed appreciably into the T = 6 analogue. These T = 5 states would also be described as linear combinations of the χ's with appropriate iso-vector coupling coefficients. ϕ_1 represents the coupling of the group $[p_{1/2}{}^3\,(g_{9/2})^{10}]$ to a $[T = \frac{9}{2},\ T_z = \frac{9}{2}]$ system while ϕ_2 represents the $[T = 1, \frac{1}{2}]$ combination. Describing the final state as $|\,f\,\rangle = |\,J^\pi = \frac{1}{2}^-,\ T = \frac{9}{2},\ T_z = \frac{9}{2}\,\rangle$ and considering the decay to proceed through the emission of $2d_{5/2}$ neutron, the width γ_n arises only from the admixture of ϕ_1 into ϕ_0, one finds

$$\gamma_n = \frac{1}{\Delta} \cdot \frac{1}{\sqrt{\hbar^2/2MR}} \left\{ \langle \phi_0 \,|\, v_c \,|\, \phi_1 \rangle \langle \phi_1 \,|\, nf \rangle \right\}$$

where Δ = average separation of T = 5 states from the analogue. The overlap $\langle \phi_1 | nf \rangle$ is observed to be 1. Exact evaluation of the matrix element $\langle \phi_0 | v_c | \phi_1 \rangle$ is complicated by the fact that the coulomb interaction v_c acts only on protons in the ϕ's which represent many-particle configurations, while the total J of the analogue state is determined by the coupling of a $p_{1/2}$ proton to a $d_{5/2}$ neutron. For an order of magnitude estimate of γ_n we can ignore this J-dependence as well as any contributions from two-particle matrix elements involving v_c. Under these assumptions the matrix elements of the one body coulomb potential may be evaluated[51]. If Λ is assumed to be of the order of 5 MeV (as suggested from consideration of the t.T potential) $\gamma_n{}^2 \approx .2\%$ of the single particle value reflecting the experimentally observed weak transition.

Internal mixing and the parameters of the analogue resonance

In the Robson theory[52] the resonance shape is governed by the asymmetry factor

$$\frac{\epsilon_\lambda - E}{\epsilon_\lambda - E - \xi_\lambda + \phi_\lambda}$$

where ϵ_λ and ξ_λ are the parameters of the R-matrix theory and refer to the analogue state $|\lambda\rangle$ while ϕ_λ describes the spreading of the analogue state due to internal mixing with $T_<$ states. If it is assumed that the relevant $T_<$ states occur in the same region of excitation as the analogue state the Wigner averaging procedure gives ϕ_λ as pure imaginary. Internal mixing effects of this type will contribute to the width but the level shift will remain unaltered.

---

(50) Nuclear Physics Division Progress Report AERE - PR/NP 10, p. 27 (1966).

(51) Lane A. M. and Soper J. M. Nuclear Physics 37, 663 (1962).

(52) Robson D. Phys. Rev. 137, 535 (1965).

In the above, $T_<$ states occur at energies considerably different from that of the analogues and averaging procedures will contribute real and imaginary parts to ϕ_λ. Denoting $T_<$ states of the same configuration as the analogue state by n> and using Robson's definition[52]

$$\phi_\lambda = -\Sigma_n \frac{\langle n|v_c|\lambda\rangle^2}{E_n - E}$$

Evaluating at the complex energy $\epsilon = E + i\epsilon$

$$\phi_\lambda(\epsilon) = -\Sigma_n \frac{\langle n|v_c|\lambda\rangle^2}{E_n - E} - i\pi\rho_n \langle n|v_c|\lambda\rangle^2_{av}$$

where ρ_n = density of $T_<$ states near the analogue resonance and may be replaced by a strength function of the form:

$$n(E) = \frac{W/\pi}{(E_n - E)^2}$$ where W is the mean absorption potential.

Order of magnitude estimates give $\mathrm{Re}\phi_\lambda \approx 16$ keV while the internal spreading width is ~ 1 keV. In view of the approximations implied we cannot attach too much significance to these numerical values. We note that while $\mathrm{Im}\phi_\lambda$ contributes in general to the spreading width of the analogue resonance, inclusion of internal mixing may reduce the overall shift factor if $T_<$ states considered are well below the analogue.

Application of analogue resonance theory to the $^{207}Pb(p,p')$ reaction (A. M. Lane and S. Ramavataram)

Recently an interesting experimental study[53] has been carried out on the decay of the 0^+ analogue resonance corresponding to the ground state of ^{208}Pb. In addition to the elastic scattering process the decay of the analogue resonance via proton inelastic scattering leading to low-lying levels of ^{207}Pb has been investigated, and the total and partial widths have been estimated.

An attempt has been made here to examine these estimates from the point of view of a comprehensive theory of analogue resonances[54]. According to this theory the total width Γ is given by

$$\Gamma = \sum_c \Gamma_c + W_o$$

where Γ_c is the partial width for channel c. The summation over c includes all possible open channels. W_o arises from the mixing of the analogue state with the neighbouring $T_<$ states. While the exact expressions for these quantities are rather complicated one can by making the random sign assumption[55] obtain the results

$$\Gamma = -2\mathrm{Im}\,[\Sigma\, \gamma_{\lambda c}^2 (S_c - b_c + iP_c)\{1 + (S_c - b_c + iP_c)R^o_{cc}\}]$$

and $$\Gamma_c = 2P_c\,|\,\gamma_{\lambda c}\,[1 + (S_c - b_c + iP_c)]R^o_{cc}]\,|^2$$

where S_c = shift factor for proton channel c

---

(53) Anderson B. L., Bondorf J. P. and Madsen B. S. Phys. Letters 22, 651 (1966).

(54) Lane A. M. and Robson D. (To be published in Physical Review).

(55) Lane, A. M. (Unpublished).

b_c = boundary condition parameter of R-matrix theory set as equal to the shift factor for neutrons in the $|nA\rangle$ channel[56]

P_c = penetration factor

and R^o_{cc} refers to the matrix element of a background R-matrix R^o with a Kapur-Peierls boundary condition.

The summation over c includes in general all channels having non-zero overlap (i.e. $\gamma_{\lambda c} \neq 0$) with the pure analogue state wave function $|\lambda\rangle$. In the particular case of the 0^+ analogue state in ^{208}Bi which is under consideration here, we note that

$$|\lambda\rangle = |^{208}Bi(0^+)\rangle = T_- |^{207}Pb_{g.s} + \nu p_{1/2}\rangle$$

and hence consists of:

(a) A single particle component corresponding to $(^{207}Pb_{g.s.} + p_{1/2})$

(b) More complicated configurations in which, consistent with the Pauli principle, one of the excess neutrons in the orbits nlj = $2f_{5/2}$, $3p_{3/2}$, $i_{13/2}$, $2f_{7/2}$ and $1h_{9/2}$ could be converted to a proton. These configurations represent excited states of ^{207}Pb in which the $3p_{1/2}$ orbit for neutrons is filled by exciting a neutron from the above mentioned orbits into the $p_{1/2}$ state plus a proton (πlj) in a scattering state. They refer to the channels with $\gamma_\lambda \neq 0$ and must be taken into account explicitly in estimating the total width Γ.

Initially the calculations have been carried out using the usual definitions of R-matrix theory[57] for the quantities S_c and P_c. The shift factor b_c for neutron channels of negative energy was obtained from the appropriate recurrence relations for Whittaker functions and their derivatives[58]. The background R-matrix was assumed to be pure imaginary and was approximated by the "strong absorption" model[57] estimate for the strength function. The $\gamma_{\lambda c}$ have been obtained from the relation

$$\gamma_{\lambda c} = \frac{2j_c + 1}{2T_o + 1} \gamma_{s.p.}$$

where j_c refers to the j-value of the single particle orbit under consideration. T_o is the isospin of the target ground state and $\gamma_{s.p.}$ is the square well estimate of the single-particle reduced width. All parameters were estimated at a radius $R = 1.30 \times A^{1/3}$. The results of the calculation are summarised in Table V (overleaf).

Perhaps a closer agreement between theory and experiment may be obtained if more realistic estimates of R^o_{cc}, the shift factors and P_c are made. For instance R^o_{cc} could be obtained from the optical model[57] while the shift and penetration factors could be obtained in terms of functions suitably corrected for nuclear effects. These problems are under investigation.

(56) Robson D. Phys. Rev. 137, 535 (1965).

(57) Lane A. M. and Thomas R. G. Rev. Mod. Phys. 2, 257 (1958).

(58) Handbook of Mathematical Functions, edited by M. Abramowitz and I. A. Stegun.

TABLE V

Final state		Theory			Experiment		
J	Excn. (MeV)	Γ_p(keV)	$\Sigma_p\Gamma_p$(keV)	Γ(keV)	Γ_p(keV)	$\Sigma_p\Gamma_p$(keV)	Γ(keV)
$1/2^-$	0	30			66		
$5/2^-$	.57	19			19		
$3/2^-$	.89	32	.85	273	44	129	220
$13/2^+$	1.63	...			...		
$7/2^-$	2.34	4			...		
$9/2^-$	3.63	...			...		

(D) Experiments relating to pure Fermi decays and to theories of weak interactions (J. M. Freeman, J. G. Jenkin, D. C. Robinson, G. Murray (Manchester) and W. E. Burcham (Birmingham)

I. The beta decay of ^{10}C

(a) Excitation energies of the first two excited states of ^{10}B: These, when combined with the result for the threshold of the reaction $^{10}B(p,n)^{10}C$, allow us to infer accurate values for the positron end points in the decay of ^{10}C to the excited states of ^{10}B. The 20 cc coaxial-drifted Ge(Li) detector (Princeton Gamma-Tech Inc.) previously described(59) was used to determine the energies of the gamma-rays following the production of ^{10}C by the $^{10}B(p,n)$ reaction. The detection system with its residual non-linearity was calibrated with gamma rays from ^{22}Na (511 keV γ-ray), ^{137}Cs, ^{54}Mn, ^{46}Sc and ^{60}Co. As a check on the reliability of the calibration the energy of the higher-energy gamma ray from the ^{22}Na source was determined. The result, 1274.62 ± 0.05 keV, is consistent with the average, 1274.54 ± 0.05 keV, of a number of recent measurements in other laboratories. The results obtained for the ^{10}B gamma-rays are 718.29 ± 0.06 and 1021.78 ± 0.12 keV, making no allowance for systematic errors. After correction for nuclear recoil the corresponding values for the excitation energies of the first two excited states of ^{10}B are 718.32 ± 0.06 and 1740.16 ± 0.12 keV.

(b) The branching ratio for the Fermi decay from ^{10}C to $^{10}B^{**}$: The new Ge(Li) detector has been used to measure the relative yields of 1022 and 718 keV gamma-rays following the decay of ^{10}C. From these yields the branching ratio for the Fermi transition to the second excited state of ^{10}B can be inferred. The semi-empirical method previously described(60) has been used to obtain a relative efficiency curve for the detector. Very satisfactory self-consistency was observed in results obtained with the calibration sources ^{22}Na, ^{46}Sc and ^{60}Co, which emit pairs of gamma-rays the relative intensities of which are accurately known: the relative efficiency for the ^{22}Na pair, predicted from the result of the ^{46}Sc and ^{60}Co measurements, agreed to 1.2% with the measured value, in spite of the extensive extrapolation involved. The required branching ratio was found to be (1.433 ± 0.023) per cent of ^{10}C decays, where the error includes a 0.3% statistical contribution, 0.5% for the relative efficiency calibration, and 1.5% for uncertainty in the contribution to the 1022 keV peak from pile-up of 511 keV pulses. This result differs from the previous measurement(60) by more than the quoted error; possible sources of systematic error are now being investigated.

(c) Half-life of ^{10}C decay: The detection of positrons to obtain a decay curve was not as successful in this case as in previous work since the beta end-point is lower and contaminant activities are not so easily eliminated by the bias setting. Gamma-ray decay curves were therefore used, a window being set

---

(59) Nuc. Phys. Div. Progress Report AERE - PR/NP 11.

(60) Nuc. Phys. Div. Progress Report AERE - PR/NP 10; also Nucl. Instr. and Methods 43, 269 (1966).

on the 718 keV peak. The measurements were followed out to a region of flat background using a multiscaler system, and were analysed by the method described below. The result 19.35 ± 0.06 sec, is consistent with the two previous accurate measurements[61,62].

II. The decay $^{35}A\ (\beta^+)^{35}Cl$

This case is of particular interest because the Fermi mode of decay predominates[60]. An accurate measurement of the half-life has now been made by following the positron decay of ^{35}A formed by the reaction $^{35}Cl(p,n)^{35}A$. The result, calculated by the method described below, is 1.770 ± 0.003 sec. Published measurements on this half-life vary considerably, but this result is consistent with the three most recent[63,64,65] and improves on their accuracy.

III. The accurate analysis of beta decay data (D. C. Robinson)

The data from the ^{35}A half-life measurement were analysed by a least squares programme using the normal weighting factor, 1/y, (y = counts/channel) and also by a programme using the weighting factor 1/Y (Y = expected or computed counts/channel). This change produced a 1% difference in the half-life. Since the second weighting, although more difficult to handle, is theoretically sounder, it was used in the final analysis.

A small approximation involved in analysing decay data by fitting a straight line to the logarithms of the counts was also investigated. It was found that this too could introduce an error of approximately 1% into the half-life. This error was eliminated by writing a least squares programme to fit an exponential curve to the actual counts per channel.

For the ^{35}A data the analysis, including these two refinements, gave 1.770 ± 0.003 sec. This is to be compared with 1.780 ± 0.003 sec, the result of analysing the same data without them. Internal consistency was much better with the new programme than with the old.

(D) A study of levels in ^{19}F (B. H. Armitage, K. Gul and B. W. Hooton)

The reactions $^{19}F(p,p')^{19}F$ and $^{18}O(d,n)^{19}F$ (Q_0 = + 5.737 MeV) were studied in order to obtain more information on the energy levels of ^{19}F. For the first reaction a 60 μgm/cm^2 BaF_2 target was bombarded with 9.0 MeV protons from the Tandem accelerator and the energies of the inelastically scattered protons were measured using the broad range magnetic spectrograph. Besides confirming the existance of a number of levels previously reported we observed a new level at 5.420 ± 0.01 MeV. Fig. 12 compares the levels we observe with those observed by other workers[66-70].

---

(61) Bartis F. J. Phys. Rev. 132, 1763 (1963).

(62) Earwaker L. G. et al. Nature 195, 271 (1962).

(63) Nelson J. W. et al. Phys. Rev. 129, 1723 (1963).

(64) Janecke J. Z. Naturforsch 15a, 593 (1960).

(65) Wallace R. and Welch J. A. Phys. Rev. 117, 1297 (1960).

(66) Ajzenberg-Selove F. and Lauritsen, T. Nuclear Physics 11, 1 (1959).

(67) Silbert M. G. and Jarmie N. Phys. Rev. 123, 221(1961).

(68) Thomas M. F. et al. Nuclear Physics 78, 298 (1966).

(69) Landolt-Bornstein Tables, Supplementary Volume on Nuclear Physics (Springer-Verlag, Berlin, Germany, 1961). 6th ed.

(70) Nuclear Data Sheets, Volume 6, published by the National Academy of Sciences - National Research Council, Washington D. C.

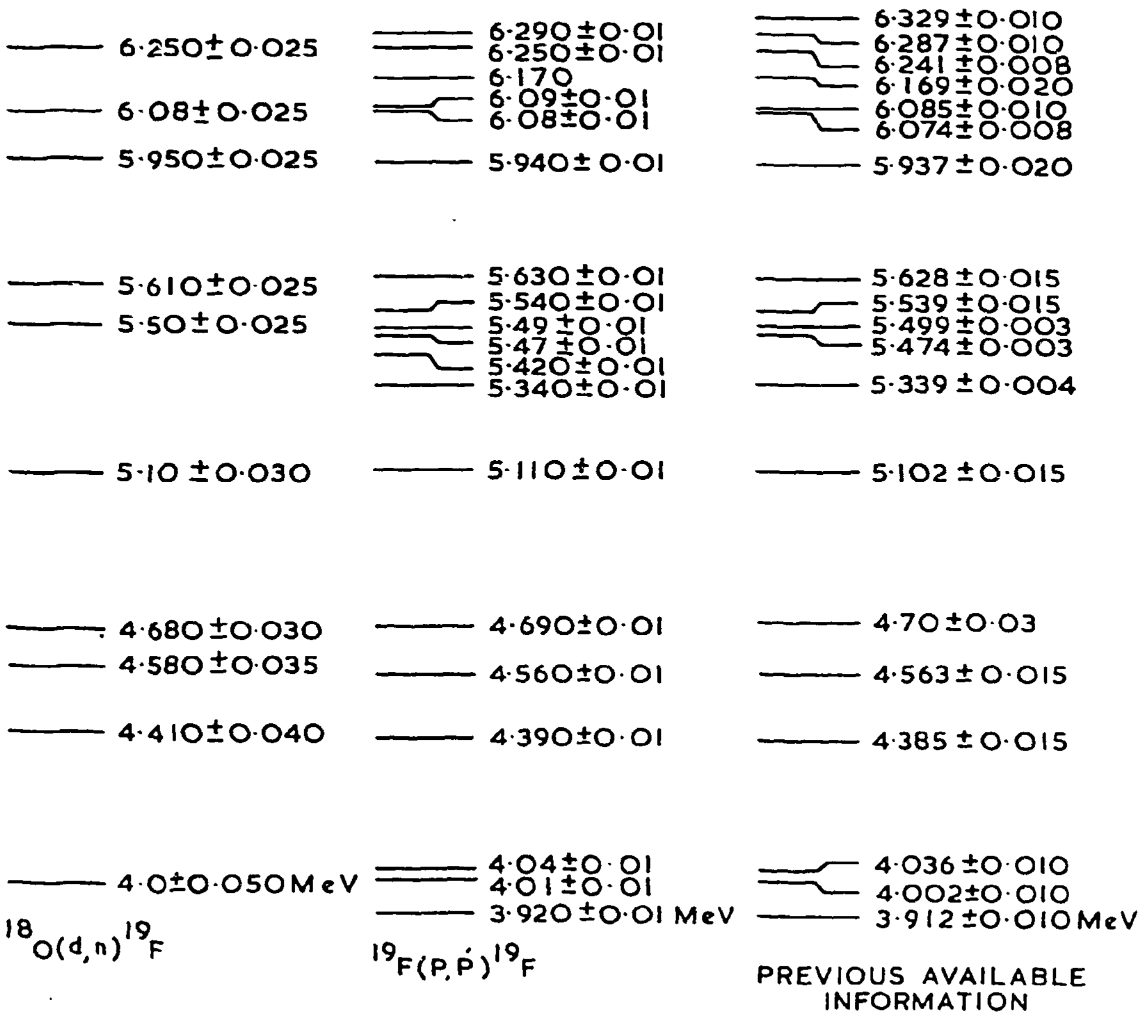

Fig. 12. A comparison between the present and previous work on the energy levels in ^{19}F.

The reaction $^{18}O(d,n)^{19}F$ was studied on the IBIS accelerator, measuring the energies of the neutrons by time of flight. A gas target containing 99.9% pure ^{18}O gas at a pressure of 30 mm Hg was bombarded with 3.0 MeV deuterons. The combined average energy loss in the nickel foil and the gas cell was about 260 keV. The energy levels of ^{19}F obtained from this reaction are also shown in Fig. 12. Fig. 13 shows angular distributions of some neutron groups from the reaction $^{18}O(d,n)^{19}F$, and lists the optical model parameters used in the DWBA stripping analysis. Many of the experimental angular distributions do not appear to give good stripping patterns, which might be expected, since at this bombarding energy considerable compound nucleus contributions would be expected.

The experimental angular distribution of the 2.790 MeV level shows a possible $\ell = 4$ stripping pattern beyond 20°. This would suggest positive parity and possible values of 9/2 and 7/2 for the spin. The value of 9/2 is preferred, since Thomas et al.[68] have excluded spins other than 5/2 and 9/2. The angular distribution to the 4.410 MeV state does not appear to be consistent with any one stripping pattern. The angular distribution of neutrons for the 5.10 MeV state agrees better with $\ell = 3$ than $\ell = 2$. This would suggest values of 5/2 and 7/2 for the spin and odd parity. No previous information on the spin and parity of the 5.10 MeV state exists. The groups at 6.080 and 6.250 MeV are strongly excited

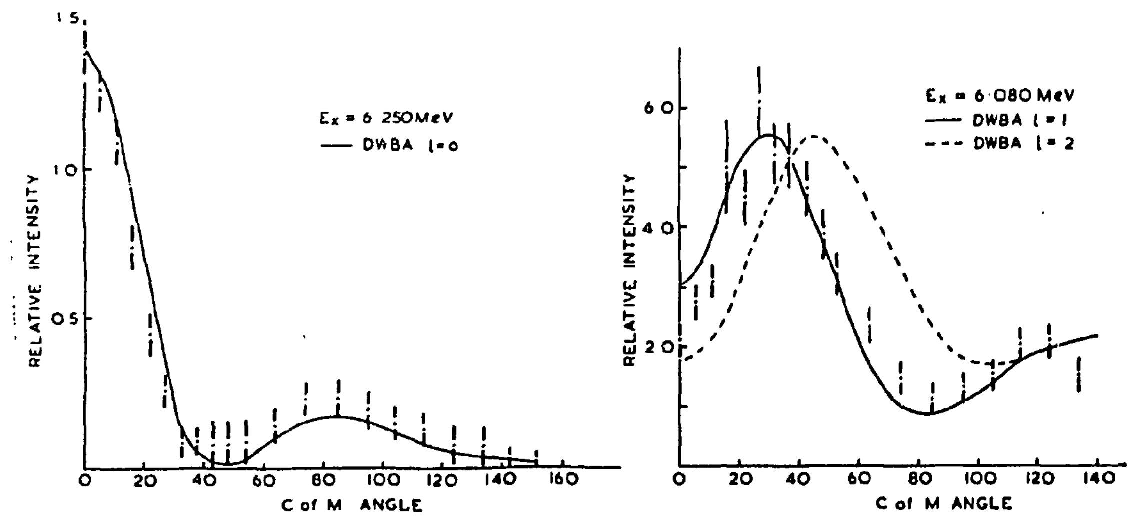

OPTICAL MODEL PARAMETERS

CHANNEL	u (MeV)	r_u (fm)	a_u (fm)	w (MeV)	r_w (fm)	a_w (fm)
$^{18}O - D$	73·0	1·40	0·70	10 0	1 40	0·70
$^{19}F - n$	49·0	1250	0 65	5·0	1250	0·65

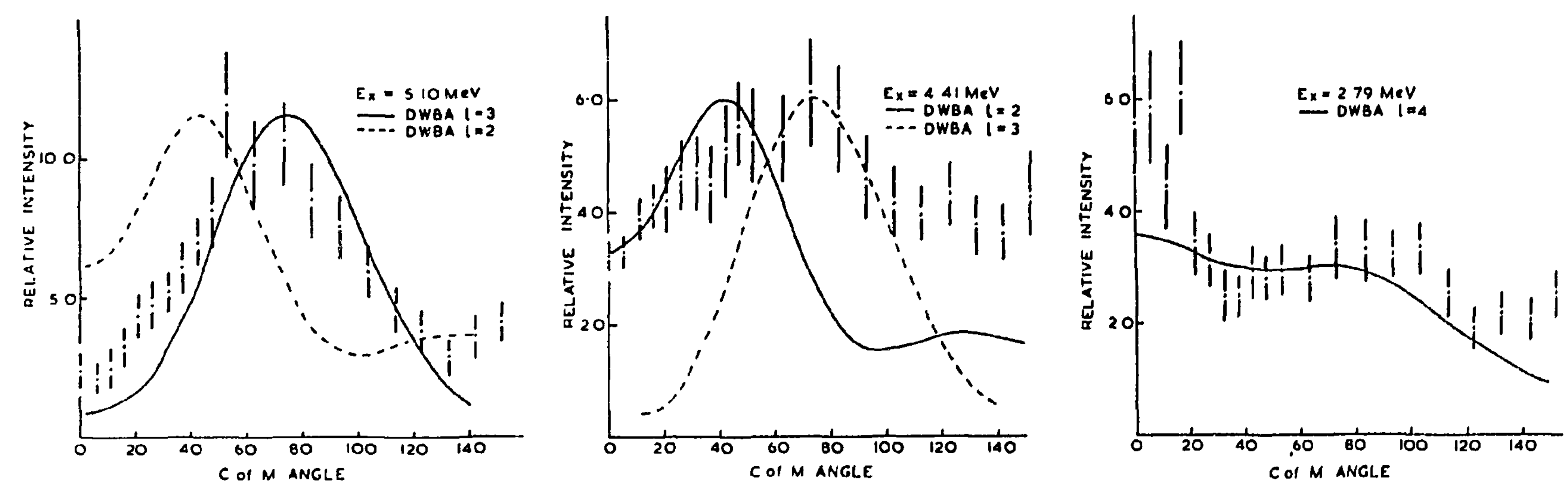

Fig. 13. Angular distributions to certain levels in ^{19}F excited in the reaction $^{18}O(d,n)^{19}F$ and the optical model parameters used in their analysis.

and show good stripping patterns. The group at 6.080 MeV could be associated with the 6.079 and 6.092 MeV levels, with reported spins and parities of $5/2^+$ and $5/2^-$ respectively[70], but the distributions suggest $\ell = 1$, giving values of $1/2^-$ and $3/2^-$ for the spin and parity, which do not agree with the previous assignments for this doublet. The group at 6.250 MeV, which fits an $\ell = 0$ stripping curve, could be the level at 6.240 MeV ($1/2^+$), but it is not resolved from the 6.273 ($5/2^+$) level. The information on the spins and parities of states in ^{19}F obtained from a study of the $^{15}O(d,n)^{19}F$ reaction is summarized in Table VI.

TABLE VI

(A summary of present results on levels in ^{19}F compared with previous work)

Present Work		Previous Information[66-70]	
Level Position (MeV)	J^π	Level Position (MeV)	J^π
2.790	$7/2^+$ or $9/2^+$	2.797	5/2 or 9/2
5.10	$5/2^-$ or $7/2^-$	5.102	
6.08	$1/2^-$ or $3/2^-$	{6.079 {6.092	{$5/2^+$ {$5/2^-$
6.250	$1/2^+$	{6.240 {6.273	{$1/2^+$ {$5/2^+$

(D) Polarization of protons elastically scattered from isobaric analogue resonances (R. K. Jolly, D. R. Maxson, G. C. Neilson and G. A. Jones)

New apparatus for polarization measurements has been developed and is being used for the determination of total nuclear angular momenta (j-values), exploiting the method recently proposed by Adams, Thompson and Robson[71]. Recent work has been reported by Terrell et al.[72] and by Veeser and Haeberli[73]. Protons are elastically scattered from medium to heavy nuclei of zero spin, via isobaric analogue resonances in the compound system. Polarization and differential cross section excitation functions are measured at suitably chosen angles over an energy range spanning each resonance of interest. The excitation function for the differential cross section reveals the orbital angular momentum ℓ, and the total angular momentum $j = \ell \pm \frac{1}{2}$ is determined uniquely from the polarization measurements. The experimentally observed cross section and polarization taken together provide additional information on other level parameters, including the total and partial widths and the resonance energy.

The measurements are being carried out by the conventional double scattering technique, using carbon analyzer foils and a 50 degree second scattering angle. Two identical polarimeters of high geometrical efficiency are mounted in vacuum on special lids on opposide sides of the scattering chamber. To compensate for spurious asymmetries arising from imperfect centering of the beam spot on the first scatterer, measurements are made with the polarimeters at equal angles above and below the beam. Other instrumental errors are cancelled by interchanging the polarimeter positions for alternate runs. The chamber lids are ball bearing mounted so that the interchange of the polarimeter positions, as

(71) Adams J. L., Thompson W. J. and Robson D. Nuclear Physics 89, 377 (1966).

(72) Terrell G., Moore C. F., Adams J. L. and Robson D. Proc. Fla. State University Conference on Isobaric Spin in Nuclear Physics, p. 333, paper C6, Academic Press, New York, 1966.

(73) Veeser L. and Haeberli W. (To be published).

well as the selection of any first scattering angle from 30 to 150°, can be accomplished without breaking the vacuum.

Because of the low efficiency in double scattering experiments it is essential that the proton beam current be as large as possible. In the initial runs with ^{128}Te (m.p. = 450°C) an excessive target deterioration was observed when more than 1/3 μA of beam current was used. This problem of target heating was solved by developing a rotating holder which permits a thin target to be spun in its own plane at 2000 rpm. The centre of rotation is displaced from the beam axis by 3/16 inch, so that with a 1/16 inch diameter beam spot the thermal energy is spread over an area 24 times as large as in the case of a stationary target. The high speed rotational motion is transmitted into the vacuum chamber by magnetic coupling. The target assembly was recently operated very successfully for five days almost continuously.

Polarization measurements have been made for one isobaric analogue resonance at E_p = 3.58 MeV in ^{54}Cr (p,p_0) scattering and for one at E_p = 7.99 MeV in ^{128}Te (p,p_0) scattering. The ^{54}Cr (p,p_0) polarization excitation function is of the expected shape and leads to a tentative $p_{1/2}$ assignment for the resonance. The polarization excitation function for the ^{128}Te (p,p_0) resonance corresponding to the isobaric analogue of the ^{129}Te ground state is shown in Fig. 14. The experimental points are relative values normalized to an appropriate theoretical curve based on Fig. 4 of Adams et al.(71). The only possible spin assignment for this $\ell = 2$ level is $j = 3/2$, in agreement with the assignment $d_{3/2}$ deduced from $^{128}Te(d,p)^{129}Te$ measurements(74). A computer program(75) is available and will be used for detailed analysis of the results.

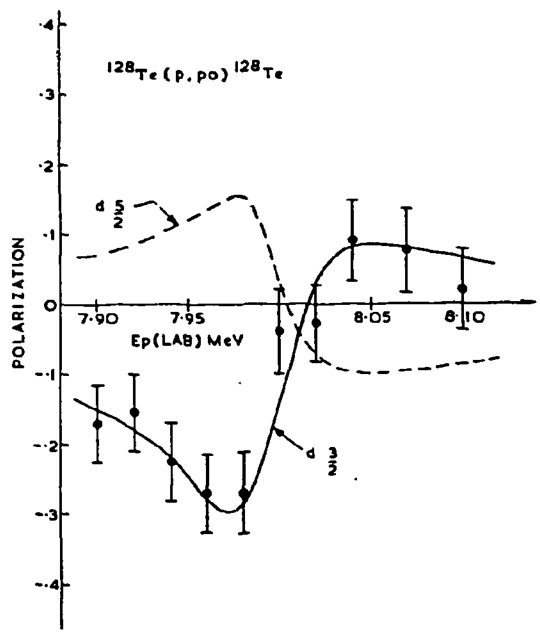

Fig. 14. Polarisation excitation function for $^{128}Te(p,p_0)^{128}Te$ scattering at a laboratory angle of 140°. The theoretical curves shown assume a total width ~ 80 keV.

The polarization measurements using targets of ^{54}Cr and ^{128}Te have provided a sufficient test of the experimental setup to demonstrate that many nuclear levels can be investigated successfully with no further refinement of the instrumentation. Similar measurements are proposed for several other nuclei and suitable targets have been obtained. It is planned to report the ^{54}Cr and ^{128}Te results in Nuclear Physics, and to submit an article describing the apparatus to Nuclear Instruments and Methods.

(D) Collective excitations in spherical nuclei via inelastic deuteron scattering (A. K. Sen Gupta, M. D. Goldberg and R. K. Jolly)

Data on both cross sections and excitation energies for the collective 2^+ and 3^- states in even-even spherical nuclei are necessary for nuclear structure calculations in the intermediate mass region(76). Extensive but rather dispersed information is available on the collective 2^+ states, but information on the collective 3^- states is scarce, possibly because most of them are at high excitation

---

(74) Jolly R. K. Phys. Rev. 136, B683 (1964).

(75) Thompson W. J. and Adams J. L. Technical Report No. 10, Flo. State University Tandem Accelerator Laboratory, January 1967 (unpublished)

(76) Yoshida S. Nuc. Phys. 38, 380 (1962); also Kisslinger L. S. and Sorenson R. A. Rev. Mod. Phys. 35, 853 (1963).

energies and are therefore somewhat difficult to study via coulomb excitation. In recent years there has been an increasing interest in the use of inelastic scattering interpreted in terms of direct interactions to study these collective excitations in even-even spherical nuclei. We have started a programme of systematic measurements of excitation energies and angular distributions for such states in the intermediate region of the periodic table. For this purpose $^{58(\times2)64}Ni$ and $^{64(\times2)70}Zn$ targets were bombarded with 11.5 MeV deuterons from the Harwell Tandem Van de Graaff accelerator, the inelastic deuterons being analysed with a Buechner-type spectrograph. Angular distributions for the collective groups were measured from 20° to 110° at 5° and 10° intervals. The cross section data are being analysed with distorted wave Born approximation (DWBA) calculations, using a deformed optical model potential. These calculations are performed for a complex coupling and include coulomb excitation effects. The parameters used are those of Perey and Perey(77). Calculations were performed using average and best fit sets of parameters for the optical potential, which yield almost identical fits to the elastic scattering data. It was found that both sets of parameters give very similar inelastic cross sections. Since average parameters are more in the spirit of DWBA calculations, it was decided to use only such parameters for all of the calculations needed for the present work. We do intend to measure the effect on inelastic cross sections of small variations of deuteron parameters (viz. those that obey the constraint VR^n = constant) around a local χ^2 minimum in the fit to the elastic scattering data.

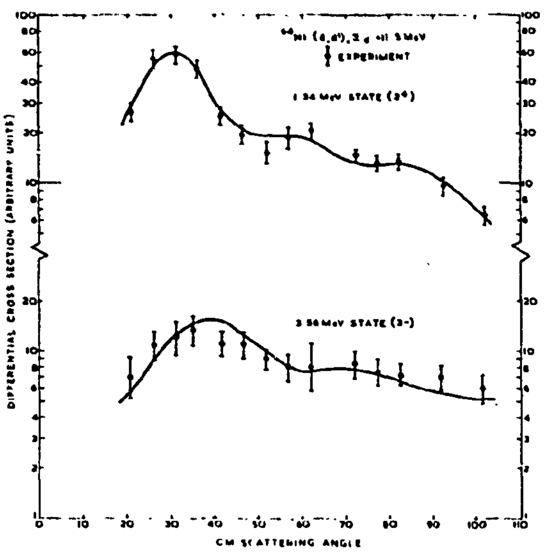

Fig. 15. A comparison of experimental cross sections with D.W.B.A. calculations for the collective 2^+ and 3^- states in ^{64}Ni.

(77) Perey C. M. and Perey F. G. Phys. Rev. 132, 755 (1963).

An example of the comparison between DWBA predictions and the experimental cross sections for ^{64}Ni is shown in Fig. 15. The agreement between the shapes of the theoretical and experimental angular distributions is quite good for both the collective 2^+ and the 3^- states.

The reduced transition probabilities are related to the experimental cross sections by the following equation

$$B(E\ell;\ 0 \to \ell) = \left[\frac{3\ Ze\ R^{\ell}}{4}\right]^2 \frac{\sigma_\ell(\theta)_{expt}}{\sigma_\ell(0)_{DWBA}} .$$

Calculations of $B(E\ell;\ 0 \to \ell)$ values await final normalisation of our cross sections.

The cross sections and excitation energies were measured using both nuclear emulsion plates and position-sensitive detectors in the focal plane of the spectrograph. Results accumulate so much faster using the position-sensitive detectors that it is planned eventually to span the whole length of the focal plane with these devices.

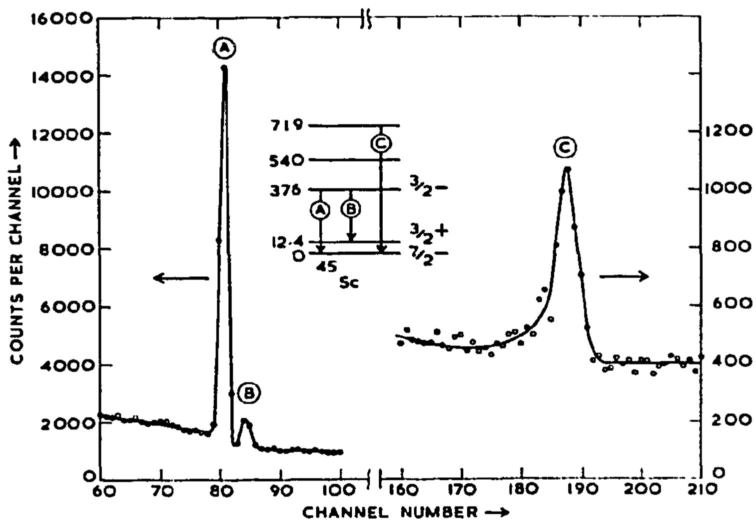

Fig. 16. Gamma-rays from coulomb excitation of levels in ^{45}Sc by 25 MeV ^{16}O ions. $\theta = 54°$.

(D) <u>Coulomb excitation of ^{45}Sc (M. D. Goldberg and B. W. Hooton)</u>

Coulomb excitation of levels in ^{45}Sc produced by oxygen ions of 15 to 25 MeV has been observed using a Li-drifted germanium detector. Measurements on thick targets of Sc and Fe were made at 0°, 90° and 54° (the zero of P_2 (cos θ)). The spectrum (Fig. 16) showed evidence of known levels at 376 and 719 keV. The B(E2) values for exciting these levels were determined by comparing the yields with that of the 842 keV level in ^{56}Fe, for which B(E2) is known(78).

Preliminary results, using an approximation for the effective target thickness, are B(E2) = 7.7×10^{-3} and 9.2×10^{-3} ($e^2\ 10^{-48}\ cm^2$) for the 376 and 719 levels respectively.

(D) <u>Lifetimes in ^{30}Si and ^{34}S measured by the doppler-shift attenuation method (W. M. Currie and A. K. Sen Gupta)</u>

Since the preliminary account of this work which was given in the last progress report we have been largely concerned with the analysis of the data and the elimination of systematic errors.

The twin target method we use(79) is illustrated schematically in Fig. 17 (overleaf). T1 and T2 are respectively the unbacked and backed targets, D1 and D2 the corresponding particle detectors. The beam passes first through T1, then through T2 and its backing. Gamma-rays from both targets are therefore

---

(78) Stelson P. H. and Grodzins L. Nuclear Data 1, 21 (1965).

(79) Nuc. Phys. Div. Progress Report AERE - PR/NP 10, p. 35 (1966).

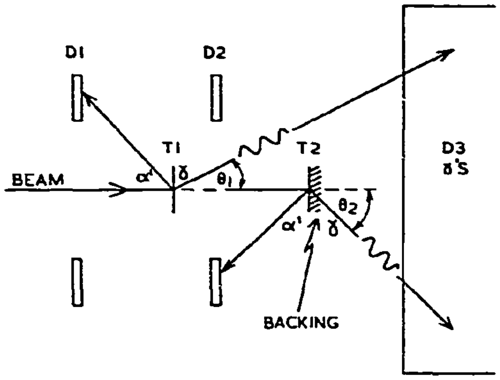

Fig. 17. Schematic diagram of the twin target arrangement for Doppler-shift attenuation work. D1 and D2 are the particle detectors, T1 and T2 the targets and D3 the gamma-ray detector. T2 is backed. It is clear that the range of possible values for θ_2 is greater than that for θ_1.

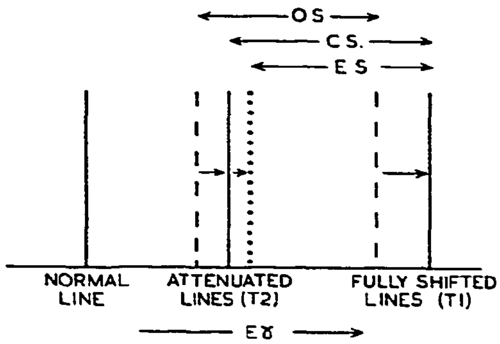

Fig. 18. Simplified illustration of the corrections which must be applied to the Doppler-shift results. The arrows indicate the directions in which the corrections move the peaks. O.S. is the observed shift, C.S. the corrected shift (after allowance for geometrical effects) and E.S. is the effective shift after large angle nuclear scattering has been taken into account.

detected in the fixed γ-ray detector D3 and identified by a time coincidence with the particles detected in either D1 or D2. The difference in the observed energies between the γ-rays from the two targets is measured.

Since the γ-rays have been observed in a NaI(Tl) detector it is the centroids of the photopeaks which are extracted from the raw data. The positions of these centroids are illustrated by the broken lines in Fig. 18, which shows a magnified part of the γ-ray energy scale. The normal line shown in this figure is just the position of the γ-ray photopeak when no doppler shift has affected it. The other solid lines indicate the centroids which would be observed in the ideal case where the detectors and targets were all confined to points on the beam axis. The main point to be noted is that the geometric and kinematic effects which arise from the finite size of the targets and detectors affect the T1 and T2 centroids differently, i.e. there is a systematic error which must be estimated and corrected. The main reason for this is the fact that the possible values of θ_2 cover a wider range than those of θ_1. Hence the observed shift (O.S.) is not equal to the corrected shift (C.S.). In Fig. 18 the arrows indicate the sense of the corrections which must be applied.

A further correction may be needed if large angle scattering at low recoil energies is significant[(80)]. Allowance for this effect is equivalent to making a correction to the centroid for the attenuated γ-ray line, indicated by the dotted line in Fig. 18. This leads to a final effective shift (E.S.) from which the lifetime may be derived if the stopping power function for the backing material is known.

The geometrical and kinematic corrections are being applied through the use of a computer program written by Dr. C. H. Johnson at Oak Ridge. For the scattering corrections we are making use of a program developed by Drs. Youngblood, Baker, et al. at the Argonne National Laboratory.

(D) Lifetime studies by the doppler-shift attenuation method (W. M. Currie, L. G. Earwaker and B. W. Hooton)

The lifetimes of levels in ^{38}A, ^{40}A and ^{33}P are being measured by the twin-target doppler-shift technique described in Progress Reports Nos. 10 and 11. In all cases the levels have been populated by the (α,p) reaction, using the doubly charged ^4He beam from the 5 MV Van de Graaff, and the γ-rays have so far been detected in a 3 in. × 3 in. NaI(Tl) crystal. The spectra are recorded on a PDP 8 computer

(80) Blaugrund A. E. Nuc. Phys. 88, 501 (1966).

which has been programmed as a multichannel analyser capable of accumulating eight 256-channel spectra simultaneously. This allows us to record pairs of γ-ray spectra from up to four excited states at one time.

The (α,p) reaction is useful for doppler-shift work because of the sizeable momentum transfer and the fact that in most cases the γ-ray background is low, but detection of the γ-rays in NaI(Tl) imposes statistical limitations which necessitate very long runs if the attenuation of the shifts is to be measured with any accuracy. The twin target technique is intended to increase the feasibility of such long runs (several days) by reducing the systematic errors arising from gain changes. Even when this technique is combined with stabilisation to maintain good resolution and line shape it is found that the system must still have fairly good intrinsic stability if shifts < 1% are to be determined reliably. In these recent measurements stabilisation was accomplished through the use of a ^{24}Na source, a β-detector and some additional electronics. Fig. 19 illustrates some results for the 2.17 MeV level in ^{38}A, where the resolution and line shape have been affected by gain changes which were almost too much for the stabilisation system.

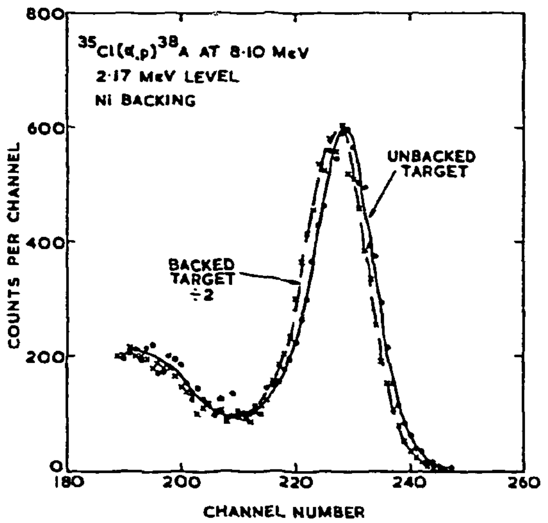

Fig. 19. Fully shifted (unbacked target) and partially shifted (backed target) photopeaks from the decay of the 2.17 MeV level in recoiling ^{38}A nuclei. The reaction ^{35}Cl(a,p)^{38}A at 8.1 MeV produces a full Doppler-shift of ~0.95%. With the Ni backing the observed shift is ~ 0.45%.

Because of such problems only rough results have so far been obtained for the Argon isotopes. They are 4×10^{-13} and $\sim 10^{-12}$ sec for the first excited states (2^+) of ^{38}A and ^{40}A respectively, and 1.0×10^{-12} sec for the second excited state of ^{38}A (spin not known).

For ^{33}P insufficient data were obtained for any lifetimes to be extracted. Our results to date serve only to confirm the provisional level scheme proposed recently[81] for this nucleus. Fig. 20 (overleaf) shows two γ-ray spectra obtained in coincidence with the proton groups for the 1st and 2nd excited states. The small peak at 0.41 MeV in the lower spectrum may be produced by a cascade from the 1.81 MeV level.

(G) A nuclear physics beam line for the variable energy cyclotron (T. H. Braid and B. W. Ridley)

The first extracted beam from the V.E.C. was obtained in June 1966, and its regular use for chemistry and metallurgy experiments commenced in November. To serve the needs of nuclear physics users for an interim period, while a high resolution facility is under consideration, it was decided in October 1966 to set up a medium resolution beam line containing a scattering chamber. A 26 inch scattering chamber with angular precision of 3′ of arc built for the proton physics group some 7 years ago for use on the P.L.A. was made available for this purpose[82]. Installation of this chamber in the V.E.C. laboratory together with the necessary beam line hardware, according to the scheme shown in Fig. 21 (see page 33), was completed in April 1967. Preliminary scattering experiments with 40 MeV ^{4}He and 53 MeV ^{3}He beams were carried out in the chamber at the end of April.

The energy spread of extracted beams from the cyclotron is typically 0.4 to 0.6% F.W.H.M., as measured with a Si(Li) detector. However, by using the bending magnet (see Fig. 21) as a beam analysing magnet, with slits 0.03 inches wide at positions A and B respectively, ^{3}He and ^{4}He beams were obtained in the scattering chamber with energy spreads of about 0.1% F.W.H.M. Beam currents

---

(81) Currie W. M. Physics Letters 24B, 399 (1967).

(82) P.L.A. Progress Report NRL/R/15, p. 51 (1961).

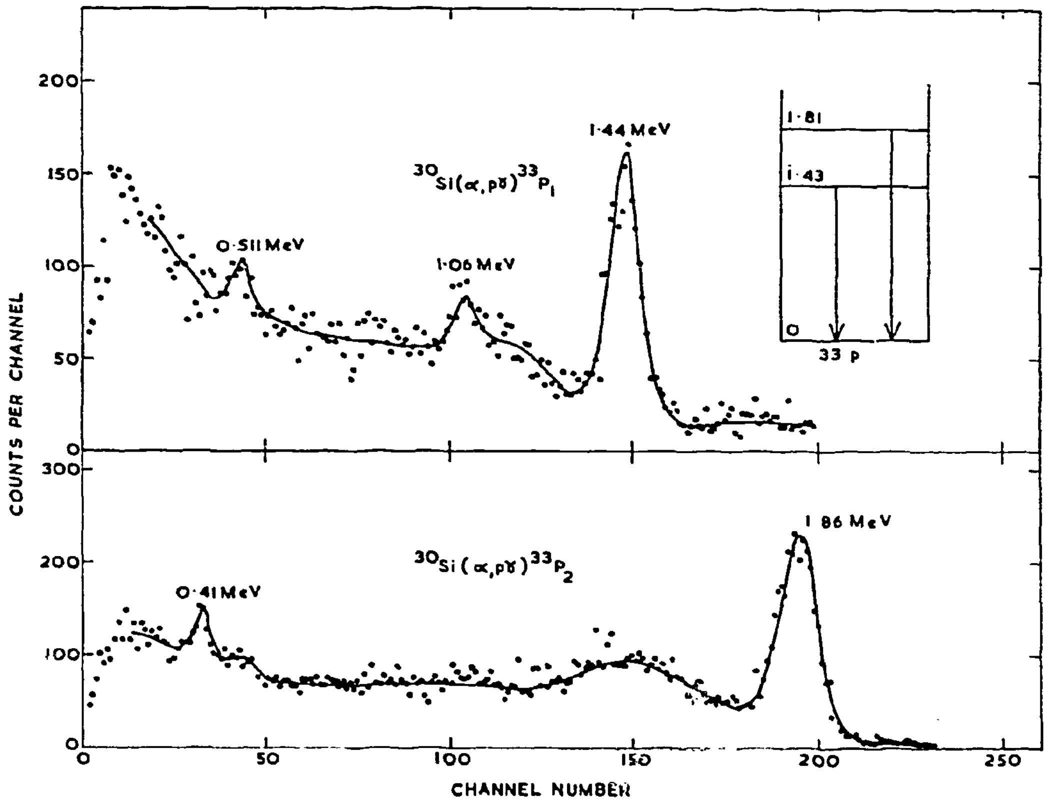

Fig. 20. Gamma-ray spectra from the first and second excited states of ^{33}P excited in the reaction $^{30}Si(\alpha,p)^{33}P$. The observed energies are in fair agreement with the level energies given in ref. (81) and the small peak at 0.41 MeV in the lower spectrum suggests that there may be a cascade from the 1.81 MeV level.

measured under these conditions at various points along the beam line for a 40 MeV ^{4}He beam are given in Fig. 21. The loss of beam at aperture C was traced to a vertical displacement of the image at that point. This will be corrected by a vertical steering magnet to be placed near quadrupole Q1.

(E) Energy spectra of photoneutrons from heavy nuclei (B. H. Patrick and E. M. Bowey)

The measurements of photoneutron energy spectra from the elements Fe, As, Nb, In, I, Ta, Au and Bi for incident bremsstrahlung spectra with peak energies 28, 35, 40 and 45 MeV have now been completed. The initial results show that as the excitation energy is increased the neutron spectra show an increasing "direct" component in the region of 10-20 MeV in all the elements studied. It is expected that no further experimental data will be collected, but work is continuing on the analysis and correction of the data.

(F) (p,d) and (p,t) pickup measurements on the tin isotopes (P. E. Cavanagh and C. F. Coleman)

The results of the (p,d) measurements on the even target isotopes (see preceding progress reports) are now being prepared for publication. In two recent runs using 30 MeV protons from the Rutherford Laboratory P.L.A. the measurements on ^{118}Sn were extended out to 88°, and a series of experiments were undertaken to give information on the levels of the even tin isotopes. These were:

(1) (p,d) measurements on ^{117}Sn and ^{119}Sn.

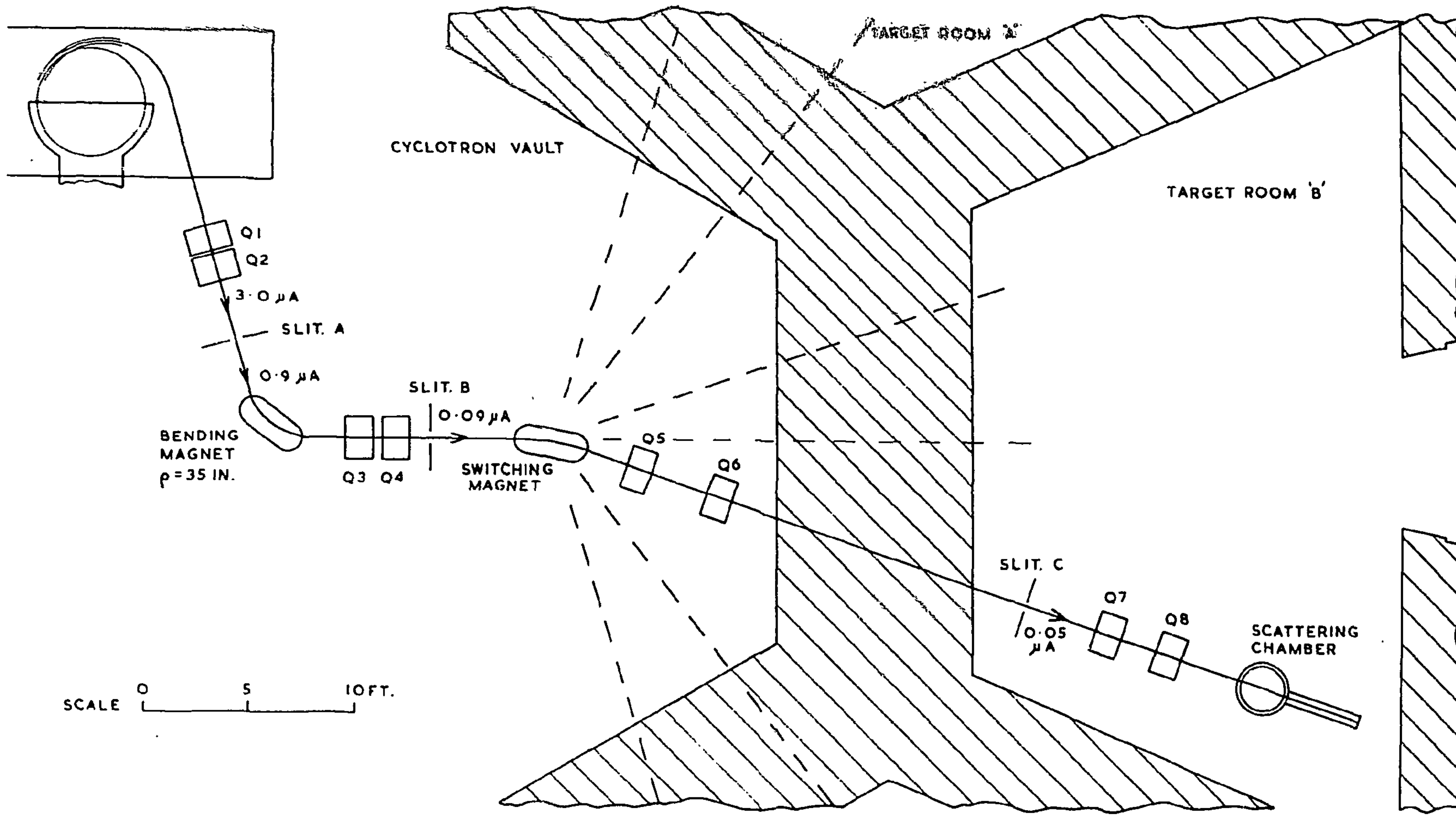

Fig. 21. Nuclear physics line on the V.E.C.

(2) (p,t) measurements at excitation of up to 5 M[illegible] the stable tin isotopes except ^{115}Sn, with a resolution ~ 70 keV f.w.h.m. for the [illegible]ts and ~ 90 keV for the odd targets. Over the first 3 MeV of excitation measureme[illegible] made at 3° intervals from 6° to 49°.

(3) (p,p′) measurements at excitations of up to 4 [illegible] the same set of targets. The resolution was ~ 55 keV f.w.h.m., and the measurements were made at 6° intervals from 14° to 80°.

The (p,d) measurements on the odd targets showed, in agreement with Schneid et al.[83], three relatively low lying 0^+ states in ^{116}Sn and ^{118}Sn, the lowest at excitations of 1.76 and 1.75 MeV, the highest and strongest (~ half the strength of the corresponding ground state transitions) at excitations of 2.55 and 2.49 MeV respectively. The two lower members of these triads were also observed in the corresponding (p,t) measurements. The maxima of the angular distributions for the (p,t) transitions to the ground states of the even isotopes move remarkably rapidly as the bombarding energy changes, from ~ 36° in our 30 MeV measurements to ~ 15° in the 40 MeV measurements of Bassani et al.[84]. This is nearly twice the shift to be expected if the position of the maximum is determined by the linear momentum transfer to the target nucleus. The 2^+ first excited states are prominent in the (p,t) spectra, and there is evidence for excitation of some of the 3^- octupole states. Others may be obscured by transitions to neighbouring levels. Fig. 22 shows the excitations of the octupole states determined from the (p,p′) measurements plotted against target mass. They show a definite minimum at A = 116, whereas the excitation energies of the 2^+ states have a broad maximum at around A = 114.

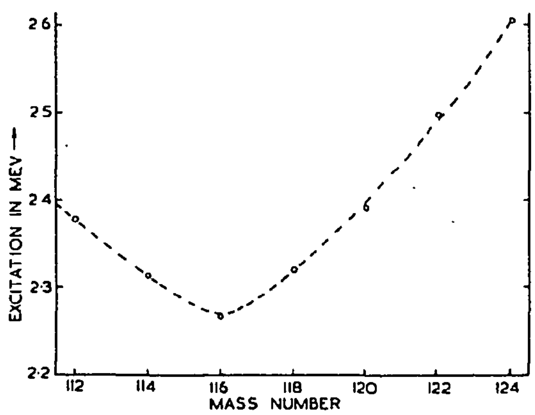

Fig. 22. Excitations of the 3^- octupole levels in the even isotopes of tin.

(F) <u>An experimental test of a new theory of pickup (P. E. Cavanagh, C. F. Coleman)</u>

Pearson and Coz[85,86,87] have recently proposed a new theory of stripping in which the deuteron is treated as a virtual neutron proton pair up to the point at which it is dissociated in the short range nuclear field. The proton is then elastically scattered. The neutron is captured into a well defined nuclear state, but acts largely as a spectator as far as the proton scattering is concerned. These authors show that this approach leads to an improved understanding of the stripping process, and in addition predicts that certain simple relations should exist between stripping angular distributions and polarizations and those for proton elastic scattering. The first of these is that the angular distribution of protons in $\ell = 0$ (d,p) stripping should be rather similar to that for elastically scattered protons of the same energy. With the additional assumption that stripping occurs preferentially in one hemisphere of the nucleus they show that the spin of the deuteron is correlated with that of the nucleus and that the outgoing protons are polarized. Consequently the difference between the differential cross sections for stripping to spin orbit pairs of j-values, $j = \ell \pm \frac{1}{2}$, for which the correlations are in the opposite sense, should be related to the polarization of elastically scattered protons.

---

(83) Schneid E. J., Prakash A. and Cohen B. L. (To be published).

(84) Bassani G., Hintz N. M., Kavaloski C. D., Maxwell J. R. and Reynolds G. M. Phys. Rev. <u>139</u>, B830 (1965).

(85) Pearson C. A. and Coz M. Nuc. Phys. <u>82</u>, 533 (1966).

(86) Pearson C. A. and Coz M. Nuc. Phys. <u>82</u>, 545 (1966).

(87) Pearson C. A. and Coz M. Ann. Phys. <u>39</u>, 199 (1966).

These predictions apply equally to the inverse reaction, (p,d) pick up, where now it is the $\ell = 0$ deuteron distribution which is expected to be similar to that of elastic scattering of the incident protons. The experimental results which have been quoted as supporting this new approach to stripping theory are all derived from low energy measurements, where there is no great momentum imbalance. It would be of interest to see if there is still agreement at higher energies, and also to see if this approach can throw light on the j-dependence we have observed in the angular distribution for $d_{3/2}$ and $d_{5/2}$ pickup at 30 MeV(88).

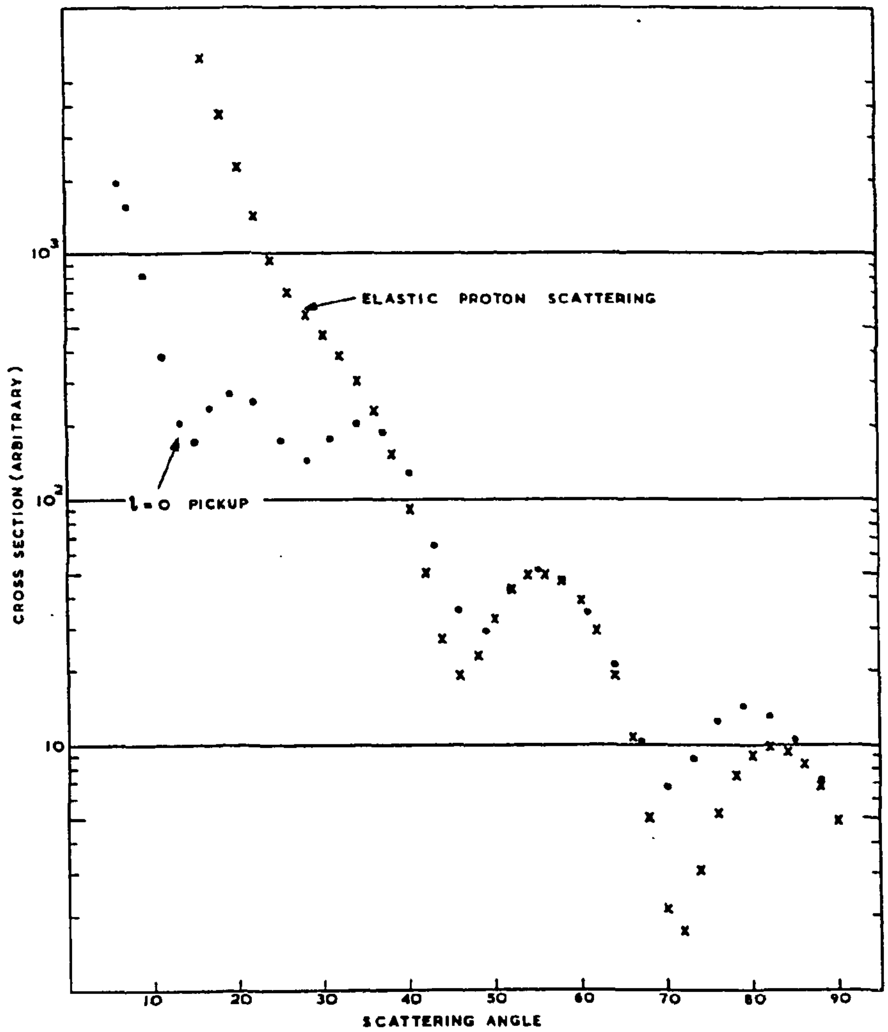

Fig. 23. Comparison of the $l = 0$ pickup distribution from the reaction $^{118}Sn(p,d)^{117}Sn$ with the elastic scattering of 30 MeV protons from ^{120}Sn.

^{118}Sn provides an ideal target for such comparisons, since all the major lines are clearly resolved. The measurements made previously over the angular range 6-49° have now been extented to 88°, using the $N^{1/2}$ spectrometer as before. The statistical errors are less than 5% on all points. Fig. 23 shows the angular distribution for $\ell = 0$ deuterons with incident protons of 30 MeV. Also shown is the angular distribution for 30 MeV protons elastically scattered from ^{120}Sn(89). The broad similarity between the

(88) A.E.R.E. Nuc. Phys. Div. Progress Report PR/NP 11 (1966).

(89) Ridley B. W. and Turner J. F. Nuc. Phys. 58, 497 (1964).

two is particularly noticeable beyond 40°, with minima occurring in both at ~ 71° and ~ 47°, while the pickup minimum at 27° corresponds to the point of inflection in the elastic scattering curve, which represents a diffraction minimum in the nuclear scattering. Close agreement would not be expected at forward angles, where coulomb scattering predominates, since break-up is assumed to occur within a distance from the nuclear surface of about the range of V_{np}, the neutron-proton interaction. The theoretical treatment truncates the coulomb potential beyond this point and the 'elastic scattering' referred to in the theoretical paper is that which would be produced by this truncated potential. Our experimental results are clearly in good agreement with Pearson and Coz's(85,86) predictions.

These authors also calculated angular distributions for the two members of a $p_{1/2}$, $p_{3/2}$ spin orbit doublet(87), and showed that if the distributions were normalised to have the same intensities at the main stripping peak the difference between them would follow - with some angular lag - the sign changes of the polarisation angular distribution for elastic scattering of protons of the outgoing energy. Thus one might expect a similar situation for the members of a $d_{3/2}$, $d_{5/2}$ doublet.

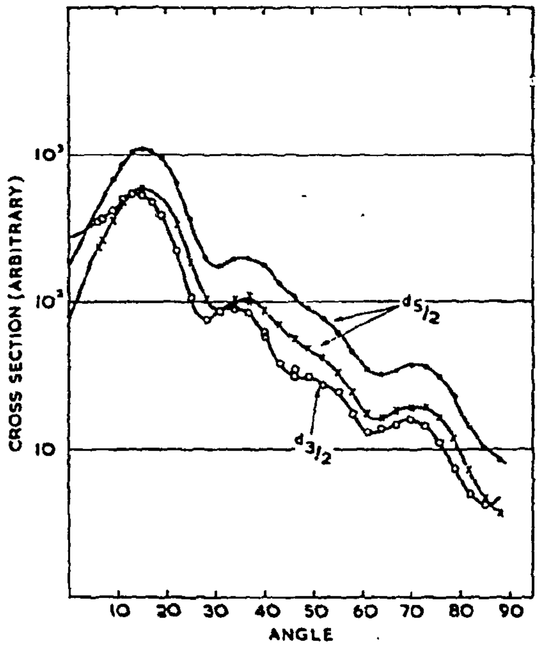

Fig. 24. Angular distributions for $d_{3/2}$ and $d_{5/2}$ pickup in the reaction $^{118}Sn(p,d)^{117}Sn$ at 30 MeV.

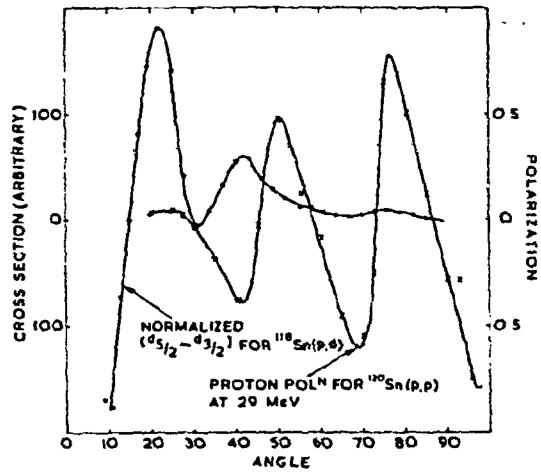

Fig. 25. J-dependence in (p,d) pickup and polarisation in proton elastic scattering.

Our experimental data for such a doublet are shown in Fig. 24. The $d_{5/2}$ distributions are very much alike, and differ appreciably from the $d_{3/2}$ distribution at forward angles, as we noted in the preceding Progress Report (PR/NP 11). The extended results show further differences near 42°, presumably corresponding to those observed by Lee and Schiffer(90) for p doublets at a lower energy and smaller angles. The difference curve obtained after normalising the peak intensities is shown in Fig. 25, along with the polarisation of elastically scattered protons observed by the Birmingham group(91). Since the positions of the zeros are very sensitive to the value of the normalising factor, while the maxima are not, we have compared the spacing of the maxima for the two curves, and find that the spacing of the second and third maxima is about 34° for the difference curve and 27° for the polarisation distribution.

---

(90) Lee L. L. Jr. and Schiffer J. P. Phys. Rev. 136, B405 (1964).

(91) Craig R. M., Dore J. C., Greenlees G. W., Lilley J. S. and Lowe J. Nuc. Phys. 58, 515 (1964).

(F) Optical model research program: elastic scattering of 30 MeV protons (A. G. Hardacre and J. F. Turner)

Elastic scattering data already obtained for a number of tin isotopes[92] and being used for an investigation of the symmetry dependence of the optical model potential, have now been supplemented by measurements on the remaining even isotopes, ^{116}Sn, ^{118}Sn, ^{122}Sn and on the odd isotopes ^{117}Sn and ^{119}Sn. These measurements have been made over an angular range 6° to 144° to the same accuracy (~ 3%) as the earlier observations. The angular range for ^{112}Sn, ^{114}Sn and ^{124}Sn has also been extended down to 6°.

The experimental data are being analysed.

(H) Neutron total cross sections (A. Langsford, P. H. Bowen, G. C. Cox and P. J. Clements (Nuclear Physics Laboratory, Oxford))

(a) Hydrogen

A description of the aims and methods of this experiment, a measurement of the total cross section in the energy range 300 keV to 5 MeV, appeared in the preceding progress report[93]. The residual uncertainty in the measurement attributed to after-pulsing of photomultiplier tubes, which was discussed in that report and also by White[94], has been overcome by viewing the plastic scintillator of the detector with two photomultiplier tubes whose outputs are taken in coincidence. Unfortunately this has at the same time introduced a smaller, rate dependent, systematic variation in the measured cross section. However, by applying calculated corrections to measurements at different beam intensities, a rate independent cross section has been obtained. Now that the major sources of systematic uncertainty are understood, further running should achieve the required accuracy, 0.2%, in the neutron-proton total cross section.

(b) Carbon

In order to be able to correct for any mismatching of the hydrocarbon samples used in the above measurement the carbon total cross section was determined in the same energy range, 300 keV to 5 MeV. The results agree with those obtained earlier[95], but depart significantly from the preferred BNL 325 (2nd Ed., Supp. 2) values. They are, however, in agreement with work at Rensselaer[96]. At this time it is not possible to rule out a 0.5% systematic error caused by non-uniformity in the carbon sample. Our results are presented in Fig. 26a (overleaf).

(c) Sodium

A further measurement of the sodium total cross section has been made in the 300 keV to 10 MeV region with the same samples as before[95], and with higher statistical accuracy. The results are shown in Fig. 26b. After the completion of the synchrocyclotron improvement programme further measurements will be made with a reduced lower energy limit in order to investigate the cross section variations reported by Hibdon[97].

---

(92) Nuc. Phys. Div. Progress Report AERE PR/NP 10, p. 42 (1966).

(93) Nuc. Phys. Div. Progress Report AERE PR/NP 11 (1967).

(94) White G. A.E.R.E. Report R 5316 (1967).

(95) Nuc. Phys. Div. Progress Report AERE PR/NP 9, p. 34 (1967).

(96) Yergin P. F. et al. Proc. Conf. on Neutron Cross Section Technology, A.E.C. CONF-660303, Book 2, p. 690 (1966).

(97) Hibden C. T. Phys. Rev. 118, 514 (1960).

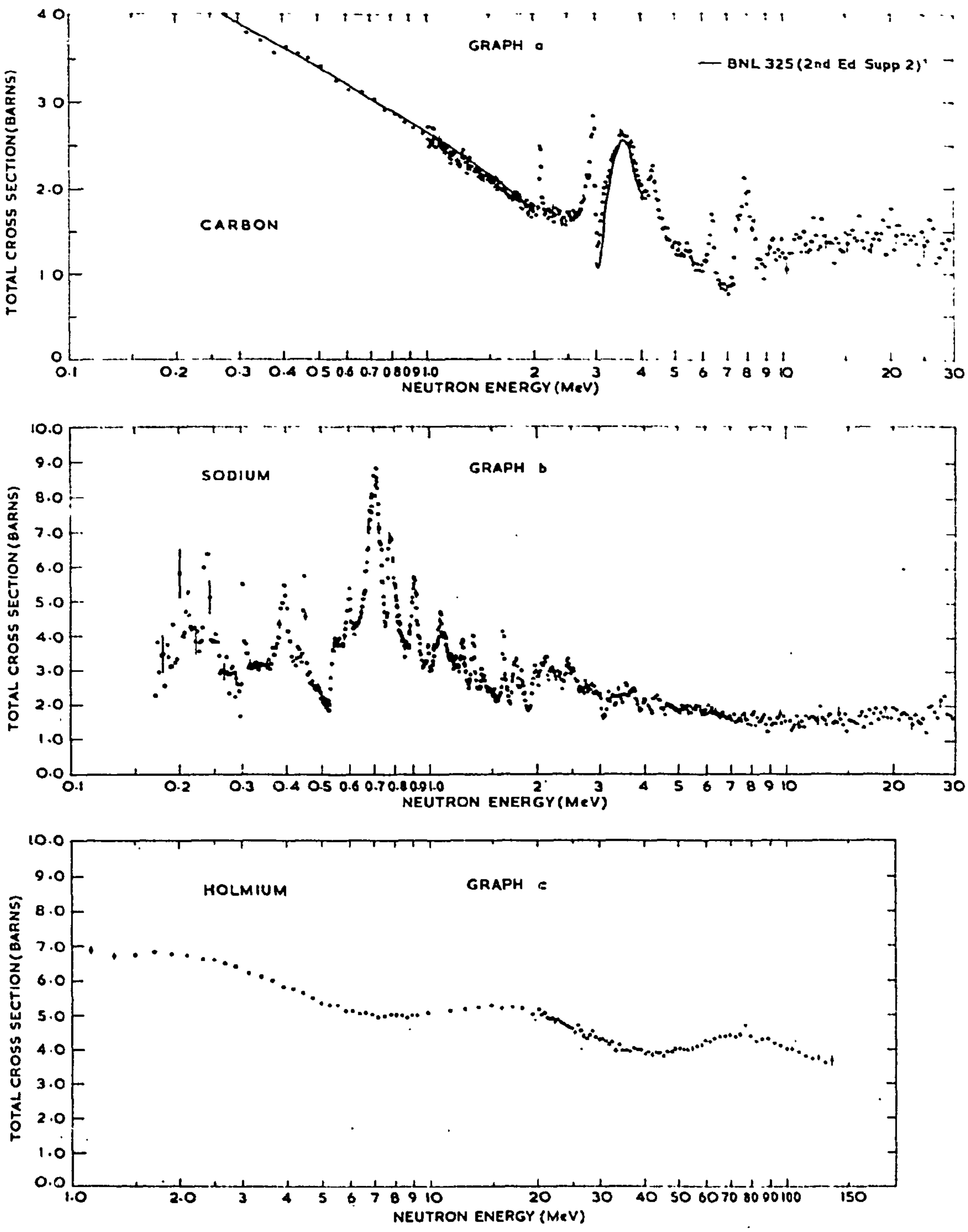

Fig. 26. Neutron total cross sections in the MeV region for (a) carbon, (b) sodium and (c) holmium.

(d) Holmium

The total cross section of a 7 cm long (0,2261 atoms bn^{-1}) sample of holmium has been measured in the energy range 2 MeV to 130 MeV and the results are presented in Fig. 26. These data were taken as part of a study to be made with Dr. H. Marshak (N.B.S. Washington) of the total cross section for longitudinally polarized holmium nuclei.

(H) Proton-proton scattering at 100 MeV (M. R. Wigan (Oxford) and P. Martin (Grenoble))

The liquid hydrogen degrader mentioned in the previous report has now been brought into operation. It reduces the energy of the external beam from ~ 145 to ~ 100 MeV with minimum multiple scattering and least low energy tail. A new technique was developed for soldering thin windows of gold-plated "Kapton" polymer film (0.003") to the hydrogen container.

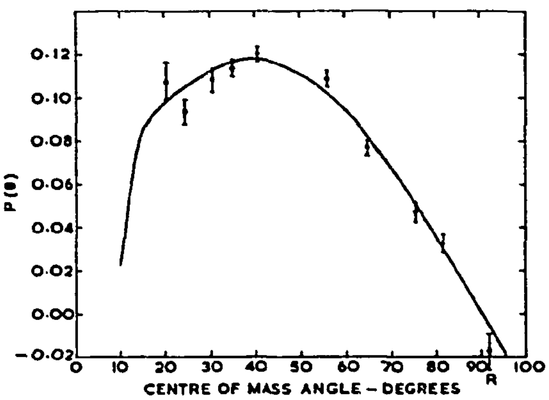

Fig. 27. Polarisation in P-P scattering near 100 MeV.

Some polarization measurements at 93 MeV have been made, and the results are shown in Fig. 27. The experimental points have a common 0.85% normalization uncertainty. The beam energy at the target centre was measured to be 93.2 ± 1.0 MeV (based on the revised Sternheimer range energy relations[98]) and the energy spread measured with a lithium drifted detector was 2.85 MeV f.w.h.m. The curves shown in Fig. 27 are the predictions of the phase-shift analyses of Arndt and Mcgregor[99].

Further polarization and cross section measurements at 97 MeV are to be made, and a new analysing system for a measurement of 'D' has been constructed.

(I) Investigation of the decay of the f^0 meson (C. Whitehead in collaboration with Southampton University, University College, London and the Rutherford Laboratory)

The analysis of the data has continued and some preliminary results are now available.

Fig. 28 (overleaf) shows the missing mass spectrum obtained to date and shows the enhancement at ~ 1250 MeV due to the f^0 meson. The solid line is the sum of a polynomial background term (indicated by the dotted line) and a Breit-Wigner resonance term with a width of 160 MeV centred at 1260 MeV, which is the best fit at the present stage of analysis.

Fig. 29 (overleaf) gives the angular distribution of the decay pions in the f^0 centre of mass system over the mass interval 1200 MeV to 1300 MeV. Points marked with a cross are those obtained from the detection of just one decay pion and the determination of its direction and momentum. The solid points are those derived from events where the directions of both decay pions were determined. The normalization between these two categories has been only approximately calculated so far and may be in error by up to 20%. The solid line in this diagram represents the distribution expected for the decay of a pure $J = 2$ resonance, which is the classification usually given to the f^0 meson, and allows it to be located in a $J = 2^+$ nonet under SU3. The absence of events around $\cos\theta^* = 0$ confirms, with enhanced statistical

(98) High energy and nuclear physics data handbook, NIRNS, Chilton (1963).

(99) Arndt R. A. and Mcgregor M. H. Phys. Rev. 141, 873 (1966).

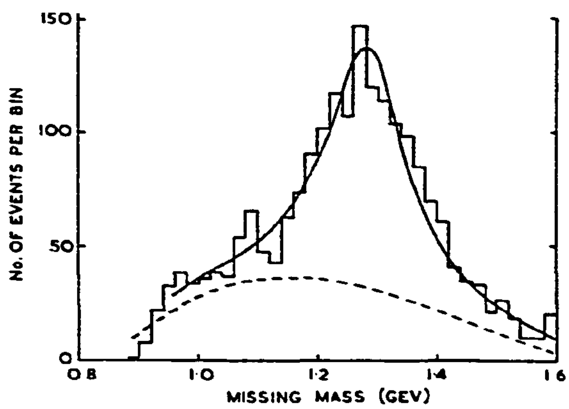

Fig. 28. Missing mass distribution from the reaction $\pi^- + p \to n + X$ between 3.1 and 3.6 GeV/c.

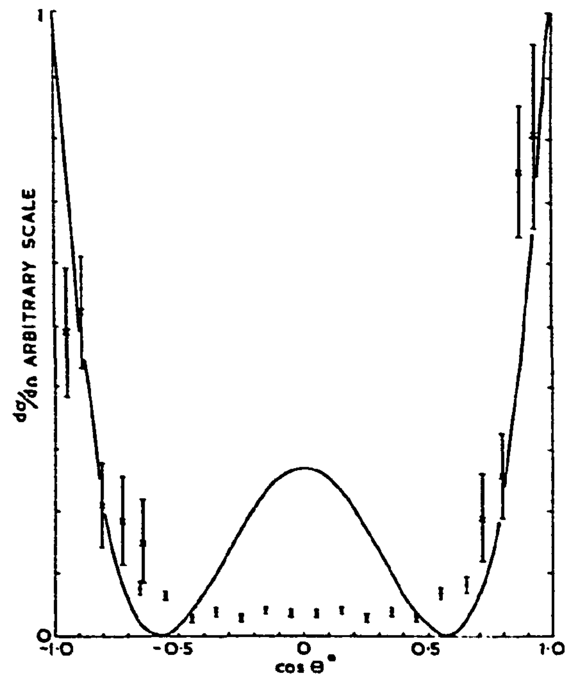

Fig. 29. Angular distribution of decay pions for the missing mass region 1.2 to 1.3 GeV.

accuracy, the findings of a number of bubble chamber experiments[100,101,102]. At present it is suggested that S-wave interference is the cause of the suppression.

(I) A study of Σ^- beta decay (I. M. Blair and A. E. Taylor, in collaboration with the Rutherford Laboratory and Queen Mary College, London)

The objective of this experiment is to measure the electron momentum – Σ^- spin correlation coefficient in the decay process

$$\Sigma^- \to n + e^- + \nu$$

as a knowledge of this quantity provides a crucial test of the current theory of weak interactions. Since the beta decay rate is only 1/700 of that for the pionic decay mode

$$\Sigma^- \to n + \pi^- ,$$

discrimination between electrons and pions is an essential part of the experiment. This is achieved by an atmospheric pressure freon gas Cerenkov counter. During the period covered by this report, tests were carried out on this counter in the meson beam from the Liverpool synchrocyclotron. It was shown that the electron efficiency was greater than 90%, and that the pion efficiency less than 10^{-5}.

---

(100) Lee Y. Y., Roe B. P., Sinclair D. and Van der Velde J. C. P.R. Letters 12, 342 (1964).

(101) Aachen-Birmingham-Bonn-Hamburg-London-Munchen Collaboration. Phys. Letters 5, 153 (1963).

(102) Aachen-Berlin-CERN Collaboration. Phys. Letters 22, 533 (1966).

The topology of the events will be studied with a wire spark chamber array using a ferrite core read-out on line to a PDP-8 computer. The last few chambers are being constructed and installed, and the programs necessary to handle the data are near completion.

The hardware and electronic logic has been installed and tested. It has been shown that most of the background arises from random coincidences in the K^+ detector. Further studies are being made to reduce the background events. It is hoped to take data within the next few months.

MISCELLANEOUS STUDIES IN PHYSICS

Mössbauer effect (T. E. Cranshaw, G. Lang, M. S. Ridout, C. E. Johnson (S.S.P.), A. P. Jain (T.R.A.) and M. Winter (Oxford))

I. Experiments with ^{119}Sn (C. E. Johnson, T. E. Cranshaw and A. P. Jain)

The study of ^{119}Sn atoms in magnetic materials has been continued. In contrast to Cu Mn alloys for which, as reported previously, a ^{119}Sn spectrum shows no magnetic splitting, Ag Mn and Au Mn show splittings which are originally approximately proportional to the concentration of Mn, but saturate at about 33 kOe for 15% Mn in Ag and 10% Mn in Au.

In Pd Fe alloys the ^{119}Sn nuclei lie in a broad distribution of fields, whose magnitudes are approximately proportional to concentration. This is in strong contrast to the ^{57}Fe field distribution, which is quite narrow and shows a marked saturation at about 10% Fe.

Further data have been obtained on the Co Sn system. The effective field at the ^{119}Sn nuclei is nearly zero at 480° and there is some indication that at higher temperatures the field becomes positive.

II. Haemoglobin (G. Lang and M. Winter (Inorganic Chem. Lab. Oxford))

We have previously reported agreement between calculated and measured spectra of the low spin ferric haemoglobins, haemoblobin azide and cyanide. This work has been extended to cover the cyanate and imidazole. The spectrum of haemoglobin hydroxide has been calculated using parameters determined from published g factors. The agreement is very good for small applied fields, but poor in zero field. The disagreement may correlate with the observation that this compound has the largest spin lattice relaxation rate of all the compounds we have investigated.

Leghaemoglobin (G. Lang)

Preliminary measurements have been made on ^{57}Fe enriched soybeans prepared by P. J. Dart of Rothamstead. Acceptable spectra have been obtained from whole root nodules, indicating that Mössbauer spectrometry may be used to study the function of leghaemoglobin as well as its structure.

III. Glasses (G. Lang)

The Mössbauer spectra of several iron compounds dissolved in frozen glycerol have been observed. High spin ferric compounds all show large magnetic hyperfine splittings at 77°K and below, with hyperfine fields which vary somewhat with the anion and are all near 550 kilogauss. Potassium ferricyanide in glycerol exhibits a simple quadrupole spectrum at 77°K and magnetic structure at 4°K. The latter is considerably modified by a small applied field, and the methods which were developed for the interpretation of the haemoglobin spectra have been successfully applied to both low temperature spectra.

IV. Studies of magnetite (Fe_3O_4) and the titanium magnetites ($Fe_{3-x}Ti_xO_4$)(C. E. Johnson and S. K. Banerjee (Newcastle-on-Tyne))

Magnetite and titanium substituted magnetites have the well known spinel structure and are of great interest (a), technically, because they have very high coercivities and (b), in rock magnetism, since titanium is found in almost all proportions as an impurity in natural Fe_3O_4.

Measurements have been made at room and low temperatures of the Mössbauer spectra of synthetically prepared compounds of formula $Fe_{3-x}Ti_xO_4$ with $x = 0$, 0.2, 0.4, 0.6, 0.8 and 1.0. The spectra were split by hyperfine magnetic fields and the lines showed effects due to (a) electron hopping between Fe^{2+} and Fe^{3+} sites, and (b) local random variations of hyperfine fields at different sites, as in an alloy. The electron hopping does not occur at very low temperatures, so that its effect could be distinguished from that due to the randomness, which in general caused the lines to be very broad. The Mössbauer effect enables the oxidation states (Fe^{2+} or Fe^{3+}) of the cations, their distribution between the different sites (octahedral and tetrahedral) in the crystal, and the distortion of these sites from perfect cubic symmetry to be determined. The spectra have been analysed to determine the re-arrangement which occurs when iron atoms are replaced by titanium in those materials.

Radio pulses from extensive air showers (W. N. Charman and J. V. Jelley)

(a) The installations at A.E.R.E. and W.R.L. (Grove)

Four months have been occupied in dealing with two specific sources of interference. The serious interference from the 73.8 MHz pulsed navigational beacon was not adequately suppressed by the anti-coincidence system mentioned in PR/NP 11. Now however complete suppression has been achieved by using a synchronous gate driven from an independent receiver tuned to the beacon. It was subsequently found that the electron linac was also causing interference; the leading and trailing edges of the 2 MW 2.5 μsec modulator pulses (at 384 pulses/sec) in either of the two radio channels produced a high chance-rate with noise pulses in the opposite channel. This was eliminated by a second gate operated from the linac's pre-pulse, provided on a coaxial line between the linac and the Measehill sites. Since early April the installation has been operating in its completed form. At the time of writing, a large rate of bandwidth-limited pulses is being observed which cannot at present by traced to any effects within the equipment. Their time distribution appears to be random and their mean rate drifts only slowly during the night periods of observation. The pulses disappear if either or both of the antennas are replaced by dummy loads. A large area (6' × 4') vertical tank of liquid scintillator has been added to the equipment to search for muons in coincidence with these observed radio pulses. The installation at Grove is partially complete. Antennas, receivers, the coincidence system, and chart recorders are complete and running, but full operation awaits a beacon suppression system.

(b) Theoretical considerations (W. N. Charman and J. V. Jelley)

The recent suggestion by Rosenthal and Filchenkov[103] that nuclear and electron bremsstrahlung, particularly from the slow δ-rays associated with ionization produced in the showers, may contribute significantly to the production of R.F. radiation from large showers, has been challenged. It appears to one of us[104] (J.V.J.) that the estimates of yield from this process[103] are far too high, and that radiation from this mechanism will be quite insignificant.

Charman has considered[105] the possibility that the atmospheric electric field may contribute to the generation of radio pulses from showers. Three mechanisms are under discussion, namely (i) vertical or transverse charge separation in horizontal showers, analogous to the magnetic separation discussed by

---

(103) Rosenthal J. L. and Filchenkov M. L. Izv. Akad. Nauk. 30 [10], 703 (1966).

(104) Jelley J. V. In preparation. Harwell Report.

(105) Charman W. N. Submitted for publication in Nature.

Kahn and Lerche[106], (ii) longitudinal charge separation for vertical showers, and (iii) radiation from the ionization electrons accelerated in the atmospheric field.

(c) Joint work with Jodrell Bank

The co-operation between the Nuclear Physics Division and Jodrell Bank is continuing. The Geiger array used in the early work[107] has been replaced by an array of eight liquid scintillators designed, constructed and tested by A.E.R.E. This was carried out in order to reduce the time-jitter in the trigger system, and to facilitate the analysis of radio records obtained in the recent north-south asymmetry experiment described elsewhere[108].

Assistance, particularly on the electronics and air-shower side, is also being provided for a mobile quiet-site experiment planned by Jodrell Bank; a caravan and diesel generator set has been obtained on loan from A.W.R.E. for this work.

Cherenkov radiation in the atmosphere (W. N. Charman, J. H. Fruin and J. V. Jelley)

The studies of the servo systems described in PR/NP 11 have now been completed. In the last stages of this work a system using a fluorescent indicating lamp was devised which was fast enough to compensate for scintillations from a bright star at low elevation, and also for a 50 cycle component of artificial light reflected by haze over the town of Wantage.

A cooled image intensifier system for astronomical spectroscopy (W. N. Charman, J. H. Fruin and A. V. Hewitt)

The complete intensifier system was operated during a two-month observing period at the Royal Greenwich Observatory, Herstmonceux. Some 50 spectra of stars in the Orion association were obtained, going down to 9th magnitude; the maximum exposure at a dispersion $\sim 3Å\ mm^{-1}$ was $\sim$ 15 min. Some high time-resolution spectra of RR Lyrae variables were also obtained. Preliminary microdensitometer analysis shows that the equivalent widths for H_γ derived from the spectra of the brighter stars of the association are in good agreement with our previous conventional measurements, while our data includes results for much fainter objects.

A review article on applications of image intensifiers in microscopy has been published[109].

(C) The channelling of protons in thin crystals (G. Dearnaley, I. V. Mitchell, R. S. Nelson (Metallurgy Division) and Prof. M. W. Thompson and B. W. Farmery (University of Sussex))

Further measurements have been made of the energy and angular distribution of protons, between 1 and 5 MeV, channelled through thin crystals of silicon. It is now apparent that channelling along a crystal axis is not explained merely as a linear superposition of effects associated with those symmetry planes which intersect in that axis. Clear evidence of competition between population of the channels associated with the <110> axis and the {110} plane has been obtained from the distribution of emerging particles. This and certain other observations suggest that two forms of lattice potential must be considered, namely a ring potential around a crystal axis and a planar potential due to atomic planes. This idea is relevant to the spreading of particles out of an axially-channelled trajectory, which is of practical importance in the utilisation of channelling for ion implantation.

---

(106) Kahn F. D. and Lerche I. Proc. Roy. Soc. A 289, 206 (1966).

(107) Jelley J. V., Charman W. N., Fruin J. H., Smith F. G., Porter R. A., Porter N. A., Weekes T. C. and McBreen B. Il Nuovo Cimento 46, 649 (1966).

(108) Porter R. A., Smith F. G. and Torbitt W. S. Nature 213, 1107 (1967).

(109) Charman W. N. Journ. Roy. Micr. Soc. 86, 33 (1966).

Other measurements have revealed that inclined planar channels are populated by the scattering of non-channelled ions into a solid angle such that capture by the channel can occur. The energy distribution in this case is quite different from that in a well-oriented planar channel.

This work is now being prepared for publication.

(H) A study of the luminescence of meteoritic materials under proton bombardment (I. M. Blair in collaboration with J. A. Edgington (Queen Mary College, London))

This work (see preceding progress report PR/NP 11) will include studies of the luminescent properties of meteoritic samples as a function of temperature, and of thermoluminescent effects. During the period covered by this report the transmission of the filters has been calibrated, with the valuable assistance of Dr. E. W. T. Richards of Chemistry Division. Runs with a few selected samples have given agreement with earlier work at lower energies, and the main body of the samples will be irradiated within the next few months.

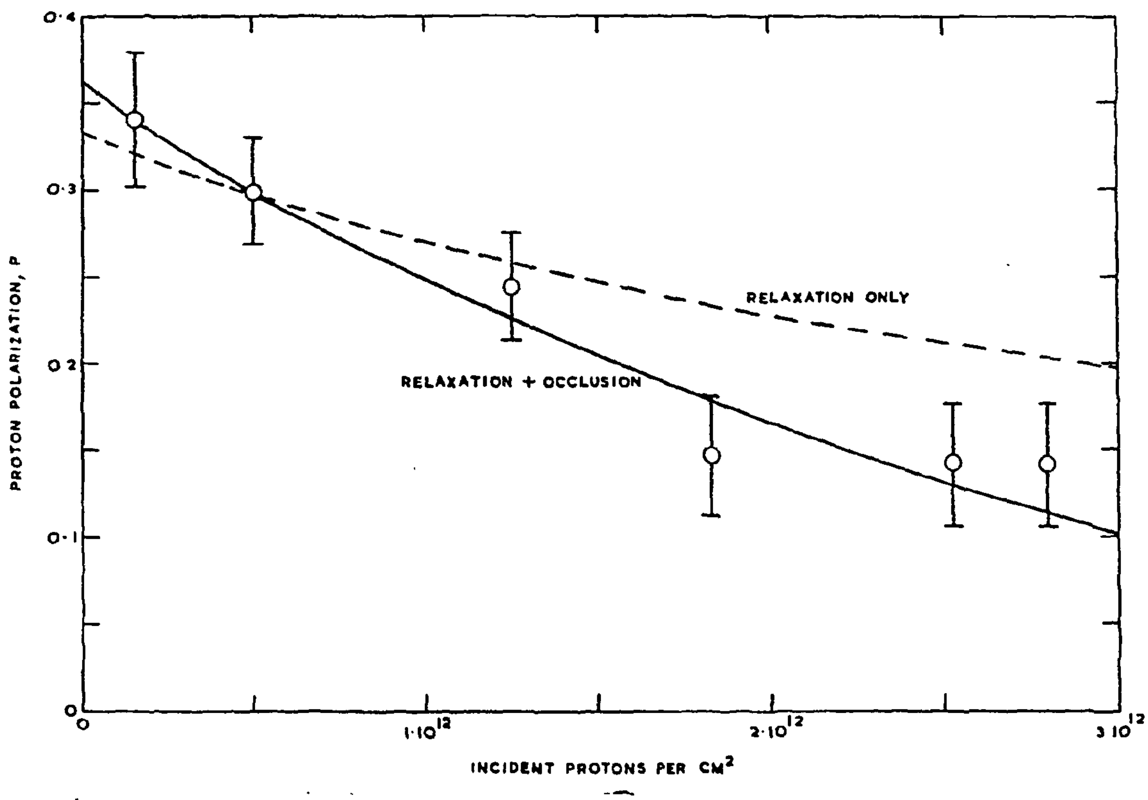

Fig. 30. Reduction in available target polarisation as a function of irradiation with 146 MeV incident protons.

Radiation damage phenomena in LaMN polarized targets (J. Butterworth (Solid State Div. AERE), J. Orchard-Webb (Exeter), J. Riley (Oxford) and M. R. Wigan (Oxford))

A reduction in the available polarization of LaMN targets caused by irradiation was reported previously(110), and the results of some measurements of this phenomenon using the Harwell target have also been given(111). These results are illustrated in Fig. 30. Further theoretical analysis has now been completed and the following conclusions reached:-

1) Approximately half the reduction is attributed to an increased proton relaxation rate (T_I) caused by damage centre build-up. The remainder may be accounted for assuming that each damage centre occludes an average of about 700 protons from the polarization process.

2) Taking into account further data obtained at the Clarendon Laboratory, Oxford on γ-irradiation of LaMN crystals, the results are found to agree within a factor of two with the Khutsishvili model(112) of "hindered spin-diffusion". The calculations will be reported in more detail in the A.E.R.E. Solid State Division progress report, and have been submitted for publication(113).

MISCELLANEOUS TECHNIQUES

Ion implantation in semiconductors (G. Dearnaley, P. D. Goode and M. A. Wilkins)

Further concentration profiles of ^{32}P implanted into single-crystal silicon have been measured under varied conditions of crystal orientation, temperature and ion dose.

At 40 keV energy, the fraction of ^{32}P ions channelled is reduced by about a factor of two when the crystal is misaligned by 1° from the <110> direction. The maximum penetration, which would determine the junction depth, is not significantly affected.

The profile of ^{32}P ions implanted along the <110> direction at 400°C shows strong lattice vibration effects which render the profile less suitable for device preparation.

Simultaneous ^{31}P and ^{32}P implantations have been carried out in order to determine for various ion energies the limiting dose at which the channelled profile is modified by radiation damage. The results should be available shortly.

100 KeV ^{32}P ions have been successfully channelled through a 0.1 micron anodic oxide layer, showing that scattering of the beam in transmission through the amorphous oxide has not prevented channelling.

A new technique of crystal orientation by means of proton channelling has been developed. 11 MeV protons from the Tandem Generator were utilised to determine the orientation of the crystal lattice with respect to the crystal normal in 0.5 mm silicon wafers to a precision of 0.02°. This has enabled good crystal alignment to be obtained for ^{32}P implantations.

In collaboration with Dr. B. Ward (on attachment from University of Surrey) projected ion ranges and profile widths for non-channelled ions in silicon have been computed for masses between 7 and 180 and energies from 40 keV to 500 keV.

We have begun measurements of electrical conductivity in phosphorus-implanted silicon wafers by the four-point probe technique, and have determined electrical donor profiles by anodic stripping. The mean range and straggling in a non-channelled 80 keV ^{31}P implantation agreed with the values calculated

(110) Nuc. Phys. Div. Progress Report AERE - PR/NP 9, p. 31 (1966).
(111) Nuc. Phys. Div. Progress Report AERE - PR/NP 10, p. 43 (1966).
(112) Khutsishvili G. R. Soviet Physics - JETP 15, pp. 909-13 (1962).
(113) Butterworth J., Orchard-Webb J., Riley J. and Wigan M. R. Proc. Phys. Soc. (To be published).

by Lindhard, Scharff and Schiott[114]. For a dose of 5×10^{14} ions per cm^2 the donor density following annealing at 700°C corresponded well with the total implanted dose. The effect of channelling on the donor profile is now under investigation, and the effect of annealing on these profiles may then be explored.

To enable the annealing of samples to be carried out without surface contamination an ultra-high vacuum furnace is being constructed. This will include a sorption pump and ion pump and will be made of metal or glass components throughout.

The preparation of lithium-drifted germanium detectors for gamma-rays (G. Dearnaley, T. C. Conlon, Mrs. D. W. Lang and I. V. Mitchell)

A coaxial detector with a volume (measured by copper stain) of over 20 cm^3 has been prepared. The energy resolution is 5.4 keV for ^{57}Co gamma-rays, and is determined by detector noise rather than trapping.

We have attempted to prepare two detectors of annular cross section by ultra-sonic boring, with a minimal volume of undepleted material. The aim was to obtain a fast response with a minimum series resistance. The lithium drift extended up to the hollow core, and no satisfactory low-injection contact has been achieved. Possibly it would be better to drift out from the core and provide a p-type contact on the more accessible outer surface.

The A.C. drift suggested by Mann[115] and Jamini[116] has been found very successful, but the procedure requires that one n-type contact should be removed and replaced by a non-injecting p-type contact. Conventional techniques have not been successful, and ion implantation is now being assessed. This has the virtue of producing a very thin window, so that a pair of detectors may be stacked together. This approach appears to be the best method of utilising the large diameter (3 in.) crystals to be produced under contract by A.S.M. Wembley.

A cluster of four quadrants cut from a 3 in. crystal has been drifted to a total volume of approximately 150 cm^3, and a cryostat has been designed and built to house the detector. The drawback to this approach is that each coaxially drifted unit has an appreciable surface dead layer, so that the overall efficiency is merely the sum of the individual detector efficiencies, i.e. multiple events involving more than one detector cannot contribute to the full-energy peak. Nevertheless, such a large detector should be most valuable, particularly at the higher gamma-ray energies.

The preparation of lithium-drifted germanium particle detectors (G. Dearnaley, A. G. Hardacre, I. V. Mitchell and B. D. Rogers)

Our objective is to make a 1 cm^2 germanium particle detector with an energy resolution for 50 MeV protons of 25 keV. A thin entrance window to the depletion layer is to be obtained by use of an Ga^+ ion implanted contact.

It has been established that this type of contact produces no serious injection when compensation by lithium drift is carried out. Techniques for crystal preparation and lithium diffusion have been developed so that reliable diodes can be produced. Four drift ovens are now in operation in a new laboratory. The chief obstacle encountered has been the variability of starting material. Hoboken germanium of 2 cm. diameter was chosen because it has shown exceptional freedom from carrier trapping. However, recent samples have shown very poor drift rates, possibly owing to excessive oxygen contamination. A sample has been supplied to A.W.R.E. for infra-red absorption analysis.

---

(114) Lindhard J., Scharff M. and Schiott H. E. Dan. Vid. Selsk. Mat. Fys. Medd. 33, no. 14 (1963).

(115) Mann H. M., Janarek F. J. and Helenberg H. W. I.E.E.E. Trans. on Nucl. Sci: NS-13, no. 3, 336 (1966).

(116) Jamini M. Brookhaven National Laboratory Report BNL 10683 (1966).

A larger detector prepared by conventional techniques has been supplied to the cyclotron group for use with 150 MeV protons. The particles travel parallel to the depletion layer, which has an area of 5.5 cm × 4.5 cm. The detector showed an energy resolution for ^{60}Co gamma-rays of about 10 keV. A collimated particle beam scanned across the detector showed the presence of a dead region at one end (see following contribution) so that the detector could not be used for the full energy particles. Again it appears that the homogeneity of the starting material is of vital importance.

(H) <u>Performance tests on a lithium-drifted particle detector (C. Whitehead and A. C. Sherwood)</u>

A solid state germanium counter intended for use with protons up to 150 MeV has recently been prepared for us by Dr. G. Dearnaley's group. The detector has dimensions 4.5 cm × 5.5 cm × 1.0 cm and was lithium drifted across the 1 cm dimension to a depth of some 8 mm as indicated by the usual copper staining technique. The 5.5 cm length allows protons with energies up to 170 MeV to be stopped within the crystal. The resolution of this detector for γ-rays is 12 keV FWHM at 1.332 MeV, the resolution being limited by break-down noise. Collection voltages in excess of 300 v produce large leakage currents, but within the quoted resolution the collection appears complete at 300 v and all measurements have been made at this voltage.

Investigations using 150 MeV protons indicated a defect in the detector, towards one end of the 5.5 cm length, in which collection was extremely poor. This defect limited investigations to protons with energies of 120 MeV, which did not penetrate to the defective region, and with these a resolution of 0.9 MeV FWHM at 119 MeV was achieved. It is believed that spread in the beam energy made by far the largest single contribution to this value. The detector response to proton energy was linear to $\sim 1\%$, the limit of the experimental technique.

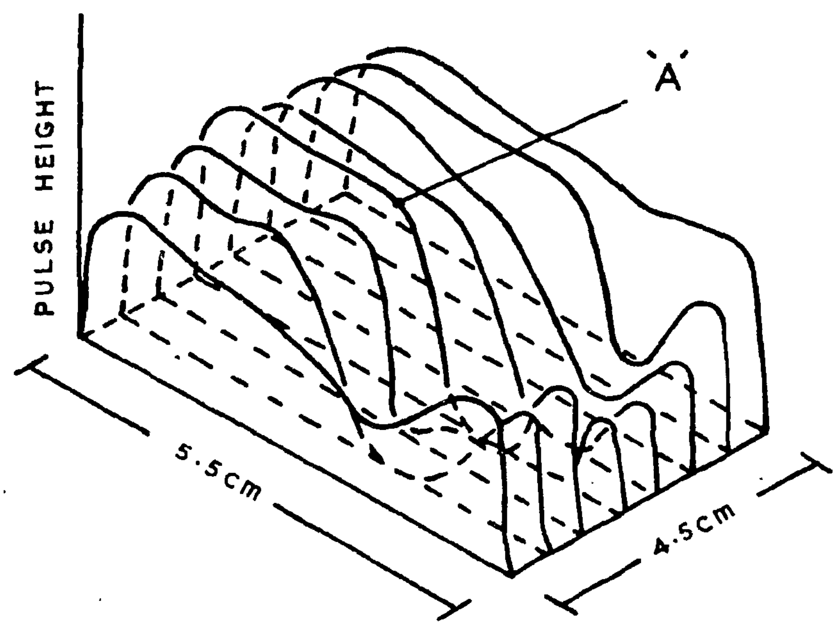

Fig. 31. ΔE pulse heights observed in scanning across largest face of detector.

In a subsequent measurement a 120 MeV proton beam collimated to 1 mm × 1 mm was used to map the detector by measuring the pulse height distributions from protons passing through the detector normal to its largest face. Fig. 31 shows the result of this mapping, the vertical co-ordinate being proportional

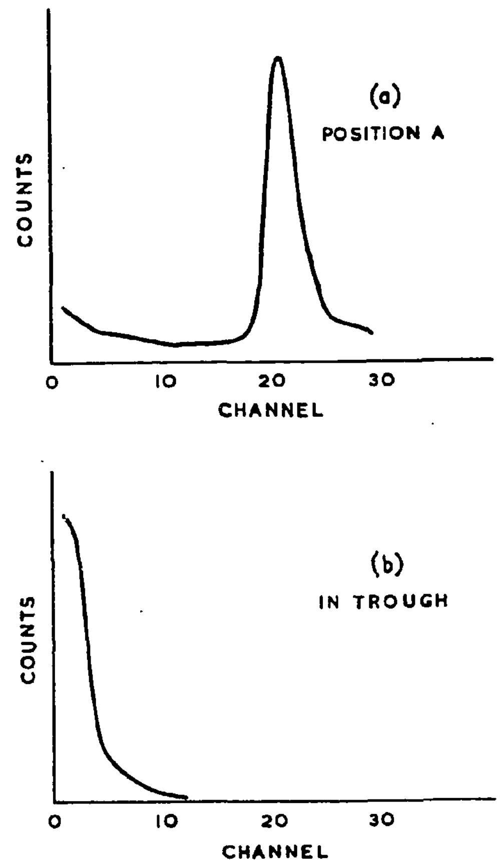

Fig. 32. ΔE pulse height distributions obtained (a) at A and (b) in the trough region indicated in Fig. 31.

to the pulse amplitude (i.e. to the energy loss of the protons). Fig. 32a shows an example of the pulse height distribution obtained at point "A" and 32b shows the distribution in the "trough". The defective volume is clearly seen in Fig. 31 and one notes particularly that the peak pulse height observed at "A" corresponds to an effective thickness of 5 mm, in contrast to the 8 mm expected from the copper staining technique.

Fig. 33 shows the spectrum of protons scattered inelastically at $\sim 40^\circ$ from a thick (7 MeV) carbon target at 120 MeV. No coincidence techniques were employed, and it is believed that the rising nature of the spectrum at lower energies is due to the relatively narrow (5 mm) width of the active region and subsequent escape, by multiple scattering, of an appreciable fraction of the protons. This is to be investigated.

ACCELERATOR OPERATION AND MAINTENANCE

Cockcroft-Walton 0.5 MV generator (A. T. G. Ferguson, F. D. Pilling, K. C. Knox, S. Waring and W. E. Sparrow)

Analysis of machine running

	hours	hours	%
Total scheduled time	607		100.0
Installation work		-	-
Scheduled maintenance and conditioning		50	8.2
Setting up ion source and beam line		60	9.9
Scheduled experimental time		497	82.0
	497	-	100.0

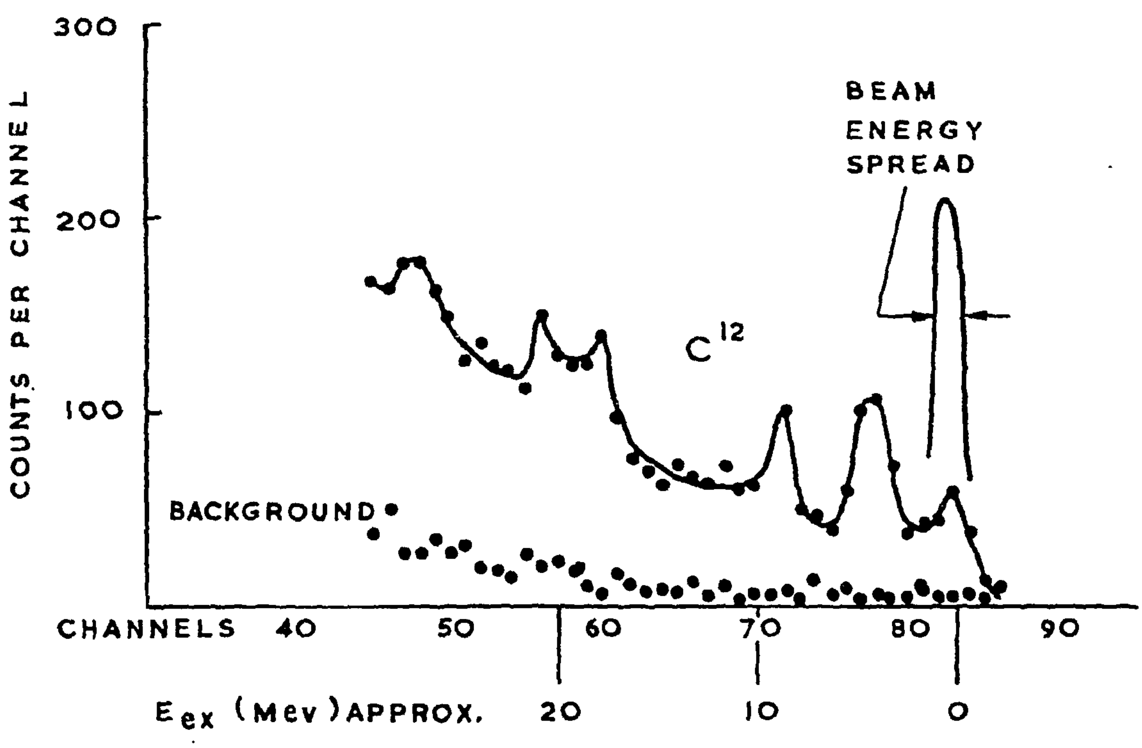

Fig. 33. Apparent spectrum of protons inelastically scattered from carbon as observed with the germanium detector.

Analysis of machine running (cont'd)

		hours	%
Experimental usage			
(1)	Metallurgy Division	238	
(2)	Electronics Division	14	
(3)	Analytical Sciences Division	144	
(4)	Health Physics and Medical Division	44	
(5)	Chemistry Division	2	
(6)	Culham Laboratory	13	
	Subtotal - other divisions and Culham	455	91.6
(7)	Exeter University	42	8.4

Modification program for .5 MV Cockcroft-Walton generator (G. Dearnaley)

Approval has now been obtained for conversion of this machine to heavy ion acceleration, in order to extend the range of ion implantation energies available at A.E.R.E. up to 500 keV for singly charged ions.

A sputtering ion source, a new accelerating tube, and a magnet capable of resolving ions up to mass 100 are now under construction. It is hoped that the conversion will be complete by October, 1967. By changing over to an R.F. ion source it will still be possible to use the accelerator for proton and deuteron beams, and the existing shielded enclosure is being retained for experiments involving high neutron fluxes.

3 MV pulsed Van de Graaff generator IBIS (D. R. Porter, F. D. Pilling and E. A. Gove)

Analysis of machine running

	hours	hours	%
Total scheduled time	1856		100.0
Installation work		-	-
Scheduled maintenance and conditioning		169	9.1
Setting up ion source and aligning beam		152	8.2
Scheduled experimental time		1535	82.7
	1535		100.0
Time lost through breakdowns		96	6.2
Available experimental time		1439	93.8
	1439		100.0
Experimental usage			
(1) Nuclear Physics		522	36.3
(2) Analytical Sciences Division		170	
(3) Metallurgy Division		22	
(4) Electronics Division		38	
(5) Solid State Physics Division		8	
(6) Culham Laboratory		2	
Subtotal - other A.E.R.E. Divisions		240	16.7
(7) Oxford University		28	
(8) Exeter University		265	
(9) Glasgow University		231	
Subtotal - University Users		524	36.4
(10) A.E.E. Winfrith		92	6.4
Machine development		61	4.2

The quartz coil core and deflection coil, quartz support rods and deflection plates in the compression system have been replaced, since the coil had become distorted and was over heating. Modifications were also carried out on the final amplifier circuit to improve the coupling efficiency.

The target assembly and pick up probe were decontaminated to reduce the background level and at the same time a new tantalum liner was fitted near the pick up probe.

A working platform is to be built for an additional beam line. It is hoped to have this completed by the end of June, 1967.

5 MV Van de Graaff generator (A. T. G. Ferguson, F. D. Pilling, K. C. Knox, S. Waring and W. E. Sparrow)

Analysis of machine running

	hours	hours	%
Total scheduled time	2343		100.0
Installation work			
Scheduled maintenance and conditioning		252	10.8
Setting up ion source and beam line		114	4.8
Scheduled experimental time		1977	84.4
	1977		100.0
Time lost through breakdowns		61	
Available experimental time		1916	
	1916		100.0

Analysis of machine running (cont'd)

		hours	%
Experimental usage			
(1)	Nuclear Physics	948	49.5
(2)	Metallurgy Division	192	
(3)	Analytical Sciences Division	102	
(4)	Health Physics and Medical Division	130	
(5)	Electronics Division	38	
(6)	Wantage Radiation Laboratory	48	
	Subtotal - Other A.E.R.E. Divisions	510	26.6
(7)	Oxford University	134	
(8)	Exeter University	70	
(9)	Manchester University	112	
(10)	Sussex University	88	
(11)	Glasgow University	32	
	Subtotal - University Users	436	22.8
	Medical Research Council	22	1.1

During this period, doubly-ionised helium beams were used for 1034 hours of the 1916 hours of experimental time. Of this total, 53% was taken up by Nuclear Physics Division, 24% by Manchester, Glasgow and Oxford Universities and the remainder by other Divisions of A.E.R.E. and the M.R.C.

In addition to the proton, deuteron and helium beams normally used, argon, neon, xenon and lithium particles have also been accelerated. This has necessitated an increase in scheduled maintenance time.

Modification (A. T. G. Ferguson, F. D. Pilling, K. C. Knox and S. Waring)

Work on the modification is proceeding satisfactorily and the majority of the components for the stack are now on site. Faulty material has caused the delivery date for the pressure vessel to be put back three weeks.

12 MV Tandem generator (J. M. Freeman, P. Humphries and F. D. Pilling)

Analysis of machine running

	hours	hours	%
Total scheduled time	1698		100.0
Installation work and conditioning		650	38.3
Scheduled maintenance		56	3.3
Setting up ion source and beam		62	3.6
Scheduled experimental time		930	54.8
	930		100.0
Time lost through breakdowns		0	0.0
Available experimental time		930	100.0
	930		100.0
Experimental usage			
(1) High Voltage Laboratory		542	58.2
(2) H.V.L., Manchester, Birmingham (collab.)		144	15.5
(3) Ion-crystal Group		48	5.2
(4) Chemistry Division		14	1.5
(5) Exeter University		60	6.5
(6) Glasgow University		60	6.5
(7) Medical Research Council		27	2.9
(8) Farnborough Space Research		11	1.2
Machine tests		24	2.5

Machine shutdown

An 8-week shutdown, the first major shutdown for 3 years, began on 8th January, 1967. During this period the following major jobs were carried out:

(1) Replacement of the accelerator tubes, which had been in use for 20,000 hours. In view of their very satisfactory performance, and insufficient evidence of overall advantages to be gained with inclined-field tubes, it was decided to use new tubes of the same "standard" design as the old tubes. The precise alignment of these tubes was greatly facilitated by the use of new variable taper units.

(2) Installation of a new stripper body and foil mechanism system with improved shut-off valves, and new components to improve the vacuum conditions at the centre terminal. Adjustable uranium/beryllium stops have also been fitted at the ends of the tubes so that the pumping speed may be increased.

(3) Replacement of the existing electrostatic quadrupole lens with a 3-section system which can if necessary be removed without moving the analyser magnet.

(4) Installation of a magnetic quadrupole lens directly below the lower accelerator tubes. It is hoped to be able to "tie" this in with the analyser magnet current.

(5) Re-alignment of the analyser magnet so that the pole pieces are accurately vertical, the horizontal axis is correctly aligned with the magnetic spectrograph axis, and provision is made for looking directly through the magnet box for both vertical and horizontal alignment.

(6) Installation of an ion pump in the stripper body.

Machine performance

Subsequent to the shutdown a modification was required to the stripper-foil operating mechanism. After an initial conditioning period, the machine has been performing satisfactorily with proton, deuteron, oxygen, and sulphur beams. Runs with deuteron energies up to 13.2 MeV ($\sim$ 0.6 μA) and oxygen ion energies up to 40 MeV ($\sim$ 0.7 μA of O^{6+}) have already been made.

Negative helium ion source development for tandem (R. H. V. M. Dawton and P. Humphries)

Cesium donor target

Experiments using cesium as a donor target were made using the H.10 mercury pool source. It was known that the pumping speed was marginal and would result in the absorption of two thirds of the negative beam, but the experiments would still be useful. The object was to investigate the effect of cesium on the voltage hold-off of the source, and to find whether good He^+ to He^- exchange occurs at energies of 30 keV. A beam of 0.75 μA of He^- was obtained at the receiver. The limitations to the current were set rather by failure of the (negative) einzel lens which follows the donor than by failure of the source to hold voltage. However, the beam and the einzel lens current were subject to slow but violent pulsations, although the ion source current drains were steady. The pulsations are attributed to unsteady cesium evaporation. The experiments show that at 30 keV the exchange ratio was satisfactory and stress two weak points, namely the einzel lens and the unsteady evaporation.

Duoplasmatron (for ion source 2)

The duoplasmatron is to provide the He^+ beam which after passage through a donor gives the He^- beam. Using 35 kV extraction, 2mA of He^+ have been obtained with satisfactory beam shape. The performance is limited by the melting of the tungsten button. Water cooling channels close to the button are being added with the hope of doubling the beam output.

45 MeV electron linear accelerator (P. P. Thomas)

Analysis of machine running

	hours	hours	%
Total scheduled time	4344		100.00
Holiday off time, Christmas 1966		117	2.69
Scheduled maintenance and installation work		371	8.55
Scheduled experimental time		3856	88.76
	3856		100.00
Time lost through breakdown		346	8.98
Machine off at users' request		33	0.86
Available experimental time		3477	90.16
	3477		100.00

Experimental usage

		hours	%
(1)	Irradiations for Analytical Sciences Div. Dr. C. Baker	51	1.47
(2)	Irradiation for R.C.C. Amersham Mr. M. Howlett	1	0.03
(3)	Experimental Runs - Cell I Mr. N. J. Pattenden, N.P. Dr. C. A. Uttley, " Dr. G. D. James " Dr. M. G. Sowerby, " Mr. M. G. Schomberg, " Mr. M. C. Moxon, " Dr. A. Asami, " Dr. B. H. Patrick, " Miss E. M. Bowey, "	2973	85.50
(4)	Experimental Runs - Cell II Dr. B. H. Patrick, N.P. Miss E. M. Bowey, "	452	13.00
(5)	Experimental Runs - Cell III Dr. R. Sinclair, N.P. Dr. M. S. Coates, " Dr. D. B. Gayther, "	2236	(64.40)*

*In the above table, Cell III running hours are less than Cell I running hours because either the Cell III users asked that the beam to Cell III be switched off or because beam transport difficulties made it impossible to provide an adequate beam at the Cell III target. The breakdown for Cell III is as follows:

	hours	hours	%
Available time	2973		100.00
Experimental time - Cell III		2236	75.20
Cell III off at users' request		435	14.64
Cell III off due to beam transport difficulties		302	10.16

General note on usage

During irradiations and when running for Cell II users, the machine is available only to one user at a time (i.e. 1 or 2 or 3) and is not available to Cell I and Cell III users (i.e. 3 and 5).

When running into Cell I, the machine is available to Cell I and Cell III users at the same time but is not available for irradiations or Cell II work.

Machine development

Machine development during this period has included the devising and installation of the following features:-

1. Irradiation facility with 'rabbit' transport.

2. Replacement of several power supply units by stabilised units.

3. Some klystron tables of improved design.

4. New electron bending magnet in Cell III together with associated supplies.

All this work was carried out during scheduled maintenance periods.

Synchrocyclotron (P. G. Davies)

Analysis of machine running

		hours	hours	%
Total scheduled time		4047		100.0
Installation work			408	10.1
Scheduled maintenance			52	1.3
Scheduled experimental time			3587	88.6
		3587		100.0
Time lost due to breakdowns			76	2.1
Available experimental time			3511	97.9
		3511		100.0
Experimental usage				
(1)	M. Wigan		998	28.4
(2)	Neutron time of flight (I) A. Langsford		664	18.9
(3)	Neutron time of flight (II) A. Langsford, M. S. Coates et al.		194	5.5
(4)	A.E.R.E./Queen Mary College I. M. Blair, J. A. Edgington		121	3.4
(5)	Royal Aircraft Establishment, Farnborough Solar Cell Irradiation		60	1.7
(6)	C. Whitehead		51	1.5
(7)	Isotope irradiations for R.C.C. Amersham		27	0.8
(8)	Health Physics and Medical Survey		2	0.1

Analysis of machine running (cont'd)

	hours	%
Machine development		
(1) Channel survey D. West	176	5.0
(2) Kim coil and R.F. measurements G. B. Huxtable	93	2.6
(3) Commissioning and testing after shutdown P. G. Davies	93	2.6
Machine not required	1022	29.5

Improvement project progress

Programme

The main shutdown date of September, 1967 still stands, although at the present time the programme is approximately four weeks late owing to difficulties with the rotating condenser.

Modulator

Manufacture of this is complete and low power circuits and interlocks have been tested. Testing at full power is about to start.

Vertical hole in the magnet

An 8.5-inch diameter vertical hole, with an 8-inch diameter vacuum-finished section at the lower end, was drilled through the magnet yoke and upper pole by Hangar 9 during the October/November shutdown. The centre of the hole was within .070 inches of the machine centre after boring was complete.

Beam tunnels

The 100 metre East neutron beam tunnel has been handed over as complete. The major part of the tunnel work was the thrust boring of a six foot tube from the 50 metre area under Street One and Building 7.21. This and the subsequent breakthrough into the Pit were completed during the October/ November shutdown. A 32-inch diameter welded steel pipe was installed in the tunnel. Work is now in progress to provide experimental facilities (e.g. cables in each area. The North beam tunnel is due for completion on 16th May.

Modifications to the pulsed beam deflection system (A. Langsford, P. H. Bowen and G. B. Huxtable)

The performance of the pulse shaping circuit has been improved by:-

(a) triggering the priming grid of the CX.1168, 80 kV thyratron, 1 μs before applying the main triggering pulse, (this grid had previously been operated under constant discharge conditions).

(b) isolating the anode circuit from the charging circuit with a choke. These modifications allow the thyratron to be operated at a higher gas pressure so that a rise time of 10 ns and a fat topped pulse of 60 ns (f.w.h.m.) is obtained without the high frequency oscillations referred to in the previous report[117].

Suitable insulated connectors, through which the pulse can be applied to the deflector plates inside the cyclotron vacuum tank, have been tested to 70 kV. Their normal operating voltage is 40 kV.

(117) AERE - PR/NP 11, p. 47 (1967).

New R.F. system (P. E. Dolley, R. Horne, G. B. Huxtable and D. Tripp)

Most of the new R.F. system is now made and is being assembled on the Hangar floor. The installation, which calls for a shutdown in September, is a month behind schedule, mainly owing to manufacturing delays on the rotating condenser. However low-power R.F. measurements will start before the end of May, and high-power tests will take place in the summer.

High voltage R.F. tests have continued on a number of components of the system, and the results indicate that the design aims will be achieved. Some of the control electronics for the new system has been designed and built.

Work on a magnetic beam-extraction coil has been suspended owing to shortage of effort. A coil of limited power rating has been tried in the cyclotron to displace the particle orbits and has yielded useful electrical and mechanical design information. Detailed calculations of particle dynamics are needed before further progress can be made.

Beam acceleration studies (J. P. Scanlon)

The studies described in the last progress report have been extended, and some firm conclusions have been reached on the generation of radial oscillation by the out-back dee system.

(a) Choice of dee shape

The dee area is limited by the maximum allowable capacity, and studies using the computer code WALKABOUT have been made to determine if there is any optimum shape within this limitation. The surprising result has emerged that a dee with a sharp cut-back is not appreciably worse than one with a smooth (curved) transition between the inner (180°) and outer (cut-back) region. The large radial oscillations generated by the former shape at the cut-back radius tend to be cancelled rather quickly, and the residual effect, almost entirely caused by coupling of the phase oscillation into the radial oscillations, is very similar for both dee shapes.

It has been decided to retain the originally planned dee shape with a sharp cut-back at $\sim$ 5" radius of 49° on each side.

Results show that radial oscillation amplitudes are closely proportional to phase oscillation amplitude. 100° peak to peak gives $\sim$ 3" amplitude.

(b) Radial oscillation suppression by magnetic field bumps

A computer code STANDSTILL, derived from WALKABOUT, was used to establish optimum field strengths as a function of radius and azimuth. Results showed that no worthwhile reduction of the phase oscillation coupling effect could be made, and this study has been discontinued.

(c) Dee voltage modulation

WALKABOUT was modified to include this, and showed that the dee voltage changes necessary to reduce phase oscillations at very small radius were far too rapid to be achieved in practice, owing to the high 'Q' of the dee system.

(d) Phase stability calculations

These have established limits for the maximum machine repetition rate which may be used. (Figures in table are in Hz).

	Abs. max. (no phase osc.)	Max. for 90° amplitude osc.
p	1480	1050
d,α	1170	820
^{3}He	1240	870

The limit is set by a phase stability "bottleneck" at about 35" - 40". By using dee voltage modulation at an earlier point in the frequency modulation cycle it would be possible to "dump" particles with large phase and radial oscillations at smaller radii, thus reducing any tank activity problems.

(e) Phase matching in the central region

WALKABOUT and phase stability calculations have shown this to be a particularly serious problem for this cyclotron. Particles accepted from the ion-source into stable orbits tend to choose initial phases leading to large phase and radial oscillation. A further study of centre geometry is being started with view to improving the phase matching, and a new orbit code SPUTNIK has been written to replace the previously used CYCLEWHEEL, which has severe limitations for studying this problem.

(f) Beam orbits at large radius

It was suggested (by Kim at Berkeley) that the performance of a beam extraction system could be improved by the use of a time dependent magnetic field perturbation at large radius (the so-called Kim coil). A new version of WALKABOUT, WALKABOUT 3, is being written to study the effects of such a perturbation on large radius beam orbits.

Ion source and central region (J. P. Scanlon, E. Wood, P. Robinson, W. H. Holland, D. Whatley and K. Done)

(a) Ion source movement

The detailed design is complete and construction is well-advanced. Some reduction of design effort was achieved by basing the design of the ion-source feed tube closely on the V.E.C. design.

(b) Electrolytic tank studies

These have continued and will provide data for SPUTNIK.

(c) Ion source

The possibility of mounting the puller directly on the ion source body has been confirmed by tests carried out in the V.E.C. A 1" long insulator of boron nitride is capable of withstanding up to 50 kV at 20 MHZ with 100% duty cycle in a field of 16 Kgauss. The design aim is 30 kV with a 50% duty cycle.

The design of three different ion-source assemblies is being finalised and the construction of a new ion-source test-rig for use on the model magnet is proceeding.

An ion-source filament supply providing [illegible]00 amps at 10 volts is under construction, and it has been established that the existing arc-pulse power supply should be adequate, at least initially.

Beam extraction (D. West)

All the computer programs necessary for the design of a regenerative beam extraction system are running on Atlas I and have been in use since January. The computation is now more than half complete. A list of preliminary parameters of the extraction system was issued at the end of February, partly as a guide to the engineering design, which is proceeding in parallel with the function design.

Measurements of the magnetic field reduction in a section of magnetic channel consisting of slabs of mild steel were made for a wide variety of steel configurations and radial positions in the fringe field of the 110" synchrocyclotron. These measurements used in conjunction with one of the computer programs will enable a realistic design of the beam extraction channel to be made.

Magnet survey (G. C. Cox)

The basic design of apparatus to survey the cyclotron magnetic field has been completed. Details are being finalised in conjunction with the Engineering Support Group, who are carrying out the design and manufacturing liaison. The design consists of a semi-automated probe carrying a search coil. Two step motors will be used to provide independent radial and azimuthal movements of the probe. Positional accuracy aimed at is .010" in both the 'r' and θ movements, giving a field accuracy of the order of 0.5 gauss in all the measurements. The search coil will be calibrated against N.M.R. probes. The automated control will be built around the Harwell Type 3016 Print-out Scaler system, in which scalers will monitor the search coil co-ordinates. The system will also monitor the integrated field values at each point of the survey, via an Integrating Digital Voltmeter. These values will be output on a typewriter and punched paper tape, together with the respective values of r and θ.

A set of temperature compensated search coils has been designed and manufacture has begun. The basic principle of shaft encoding by means of Ga As diode light emitters viewed by photocells has proved satisfactory. The outline of the logics of the system has been designed, and control equipment and necessary electronic components are now being delivered.

REPORTS AND PUBLICATIONS

REPORTS

AERE - R 5331 Neutron Energy Spectra and Angular Distributions from Targets bombarded by 45 MeV Electrons. D. B. Gayther and P. D. Goode.

AERE - R 5335 The use of Colour Film in the Study of Proton Channelling. R. S. Nelson, B. W. Farmery, G. Dearnaley and I. V. Mitchell.

AERE - R 5355 Ion Implantation Progress Meeting. G. Dearnaley.

PUBLICATIONS

CHARMAN W. N. Image Intensifiers in microscopy. J. Roy. Micr. Soc. 86, 33 (1966).

DAY R. B., DEARNALEY G. and PALMS J. M. Noise, Trapping and Energy Resolution in Semiconductor Gamma-ray spectrometers. I.E.E.E. Trans. on Nucl. Sci. NS-14, No. 1 (1967).

DEARNALEY G. Nuclear Radiation Detection by Solid State Devices. Journal Sci. Instrum. 43, 869 (1966).

EARWAKER L. G. A study of the $^{9}Be(^{3}He,t)^{9}B$ and $^{9}Be(^{3}He,^{3}He)^{9}Be$ reactions. Nuclear Physics A90, 56 (1967).

JELLEY J. V., CHARMAN W. N., FRUIN J. H., SMITH F. G., PORTER R. A., PORTER N. A., WEEKES T. C. and McBREEN B. Il Nuovo Cimento 46, 649 (1966).

LAWERGREN B. The $^{26}Mg(d,n)^{27}Al$ reactions. Nuc. Phys. A90, 311 (1967).

LAWERGREN B. The spin of the 974 keV level in ^{28}Al. Nuc. Phys. A96, 49 (1967).

LAWERGREN B. The $2s_{1/2}$ component in the ground states of nuclei in the $16 \leqslant A \leqslant 36$ region. Phys. Lett. 24B, 395 (1967).

LAWERGREN B. and MITCHELL I. V. A high resolution measurement of the $^{14}C(d,n)^{15}N$ reaction. Nuc. Phys. A99 (1967).

NELSON R. S., FARMERY B. W., DEARNALEY G. and MITCHELL I. V. The use of Colour Film in the Study of Proton Channelling. J. Mater. Sci. 2, 171 (1967).

SEAMAN G. G., LEACHMEN R. B. and DEARNALEY G. Fluctuation Studies of the (α,p) Reaction on ^{19}F, ^{23}Na and ^{31}P. Phys. Rev. 153, 1194 (1967).

IN COURSE OF PUBLICATION

DEARNALEY G. Solid State Radiation Detectors. Contemporary Physics.

DEARNALEY G. and WILKINS M. A. Crystal Wafer Orientation by Proton Channelling. Journal Sci. Instrum.

DUBOIS J. and EARWAKER L. G. A study of levels in ^{23}Mg. Physical Review.

FREEMAN J. M. Weak interactions. Encyclopaedic Dictionary of Physics, Supplementary volume (Pergamon Press).

GAYTHER D. B. and GOODE P. D. Neutron energy spectra and angular distribution from targets bombarded by 45 MeV electrons. Jour. Nuc. Energ.

JAMES G. D. Pulsed Neutron Research (Survey). Encyclopaedic Dictionary of Physics, Supplementary volume (Pergamon Press).

LYNN J. E. Neutron resonance reactions. Oxford University Press.

CONFERENCE PAPERS

Invited Papers:

DEARNALEY G. Ion Channelling. Proceedings of the Symposium on Radiation Effects in Semiconductor Components, Toulouse, 7-10 March, 1967.

DEARNALEY G. Semiconductor Detectors in Nuclear Physics Research. Proceedings of the International Seminar on Low Energy Nuclear Physics. Dacca, E. Pakistan, 16-25 January, 1967.

Contributed Papers:

4th Annual Solid State Physics Conference, Manchester, 4-7 January, 1967

DEARNALEY G., FARMERY B. W., MITCHELL I. V. and NELSON R. S. Proton Channelling in Thin Crystals.

Conference on the nucleon-nucleon interaction, Gainsville, March, 1967

WHITEHEAD C. Present and future work with the Harwell Synchrocyclotron.

Conference on Elementary Particles, London, April, 1967

BIRD L. and WHITEHEAD C. (A.E.R.E.), AULD E. G. (R.H.E.L.), CRABB D. G., OTT R. and McEWAN G. (SOUTHAMPTON UNIVERSITY), AITKEN D. K., BENNETT G., HAGUE J. F., JENNINGS R. E. and PARSONS A. S. L. (UNIVERSITY COLLEGE, LONDON). A study of the inelastic $\pi^{-}p$ interactions in the region of 3.2 GeV/c.

Divisional Staff

Division Head: Dr. B. Rose

Group Leaders:
Dr. P. E. Cavanagh
Dr. T. E. Cranshaw
Dr. G. Dearnaley
Dr. A. T. G. Ferguson
Dr. J. M. Freeman
Dr. J. V. Jelley
Dr. E. R. Rae
A. E. Taylor

J. M. Adams
B. H. Armitage
P. H. Bowen
B. P. Clear
Dr. C. F. Coleman
Dr. W. M. Currie
K. M. Diment
Dr. L. G. Earwaker
P. D. Goode
Dr. B. W. Hooton
Dr. J. H. Irvin
Dr. O. N. Jarvis
R. I. MacDonald
N. J. Pattenden
D. R. Porter
M. S. Ridout
Dr. J. P. Scanlon
A. C. Sherwood
W. Spencer
J. F. Turner
S. Waring
Dr. C. Whitehead
E. Wood

G. V. Ansell
D. A. Boyce
Miss E. M. Bowey
Dr. M. S. Coates
G. C. Cox
G. B. Dean
P. E. Dolley
Dr. D. B. Gayther
A. G. Hardacre
G. Huxtable
Dr. G. D. James
Dr. A. Langsford
M. C. Moxon
F. D. Pilling
Dr. B. W. Ridley
B. D. Rogers
M. G. Schomberg
Dr. M. G. Sowerby
D. J. Tripp
Dr. C. A. Uttley
D. West
M. A. Wilkins

Fellows, Temporary Research Associates and Attached Staff in Nuclear Physics Division

Dr. A. Asami	Attached	Japan Atomic Energy Research Institute, Tokae-Mura
Dr. M. Aslam	Attached	Pakistan Atomic Energy Commission
R. A. Bell	Attached	Oxford University
Dr. T. H. Braid	Attached	Argonne National Laboratory
Dr. W. N. Charman	Fellow	
P. J. Clements	Attached	Oxford University
Dr. T. W. Conion	Fellow	
Dr. M. Goldberg	Attached	Brookhaven National Laboratory
K. Gul	Attached	Oxford University
A. V. Hewitt	Attached	Oxford University
Dr. A. P. Jain	T.R.A.	
Dr. J. G. Jenkin	Fellow	
Dr. R. K. Jolly	Fellow	
Mrs. J. C. Lang	T.R.A.	
Dr. L. G. Lang	T.R.A.	
Dr. B. T. Lawergren	Fellow	
P. J. Martin	Attached	Laboratoire de Physique Nucleaire, Grenoble, France
Dr. D. R. Maxson	Attached	Brown University, Rhode Island, U.S.A.
Dr. I. V. Mitchell	Fellow	
Dr. G. C. Neilson	Attached	University of Alberta
C. M. Newstead	Attached	Oxford University
Mrs. S. Ramavataram	T.R.A.	
Dr. D. C. Robinson	Fellow	
Dr. A. K. Sen Gupta	T.R.A.	
Dr. W. E. Stein	Attached	Los Alamos Scientific Laboratory
Dr. R. B. Taylor	Fellow	
M. Wigan	Attached	Oxford University